DEMOCRATIC AND POPULAR ALGERIAN REPUBLIC
MINISTRY OF HIGHER EDUCATION AND SCIENTIFIC RESEARCH
ECHAHID HAMMA LAKHDAR UNIVERSITY OF EL-OUED
FACULTY OF: TECHNOLOGY

Master's Thesis

In order to obtain a diploma of an Academic Master
Department: Mechanical Engineering
Specialty: energy

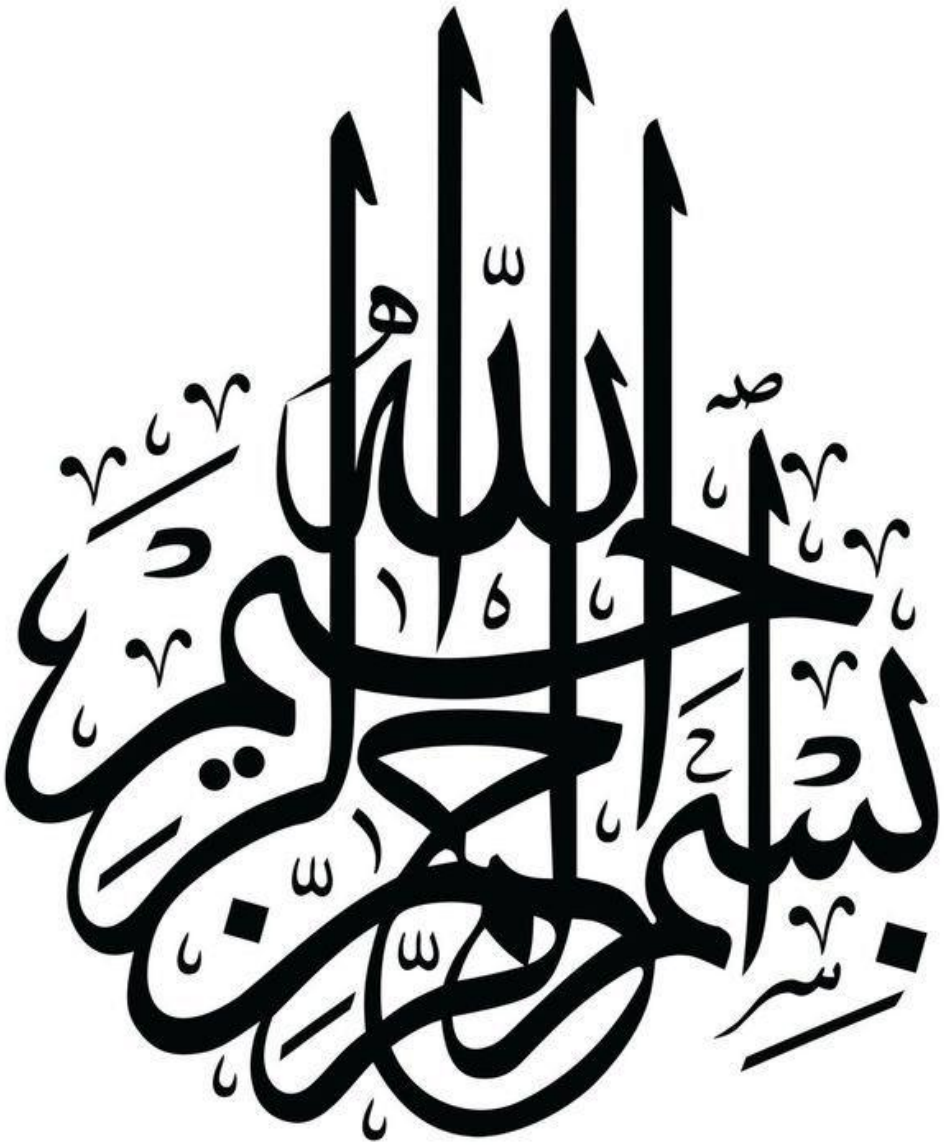
Theme

Modeling Drying Kinetics with Solar-Hybrid Storage Systems for Efficient Orange

Submitted by:
HAMAIDI Mohammed Laid
BAFFI Dia Eddine

President	**Dr . BOUHLAL Abd Elhamid**	**M.C.A**	**El-Oued University**
Examiner	**Dr . ALI Boukhari**	**M.A.A**	**El-Oued University**
Supervisor	**Dr.MENECEUR Noureddine**	**M.C.A**	**El-Oued University**

University year: 2025/ 2026


بسم الله الرحمن الرحيم

Acknowledgements

First and foremost, all praise and gratitude are due to Almighty Allah for giving us the strength, patience, and ability to successfully complete this master's thesis.

We would like to express our deepest gratitude and utmost appreciation to our esteemed supervisor,

Dr. MNASSER Nour Eddine

for his invaluable guidance, continuous support, and insightful remarks throughout the development of this research. His expertise and dedication have been crucial to the completion of this work.

Our sincere thanks also go to the President and the Examiner of the defense committee for their time, effort, and constructive evaluations that will undoubtedly enrich the academic value of this study.

Finally, we extend our appreciation to the faculty members and staff of the Faculty of Technology at Echahid Hamma Lakhdar University of El-Oued for providing a supportive research environment.

Dedication

To those who carried the torch of patience to illuminate our path toward knowledge...

To our beloved parents, whose unconditional love, continuous support, and endless prayers have been the ultimate fuel for our success.

To our brothers and sisters, for their constant encouragement and presence throughout this journey.

To our life partners, who shared our burdens and stood by us with unwavering faith and devotion.

To our dear friends and colleagues, who accompanied us through the long nights of research and shared the joy of every milestone.

We dedicated this humble piece of work to all of you, with our deepest love and gratitude.

Abstract

In light of the global shift toward renewable energy, this study addresses the intermittent nature of solar radiation by integrating thermal energy storage techniques into solar drying technologies. This thesis presents a comprehensive experimental investigation and mathematical modeling of the drying kinetics of orange slices (4–6 mm thickness, 85–90% initial moisture content) under the arid climatic conditions of the El-Oued region, southeastern Algeria, during the summer of 2026. Two advanced Indirect Solar Dryer (ISD) prototypes operating under forced convection were evaluated and compared. The first setup utilized a conventional flat-plate solar collector as a baseline reference. In contrast, the second prototype was enhanced by integrating an innovative thermal composite material within the collector, marrying the high latent heat capacity of paraffin wax with the superior thermal conductivity of aluminum shavings (PCM-ALSH). The empirical results indicated that the PCM-ALSH integrated collector attained a superior thermal peak and produced a pronounced thermal lag during solidification, prolonging effective drying activities for several hours beyond sunset. This dynamic response effectively functioned as a thermal buffer, smoothing temperature fluctuations, reducing overall drying time, and preserving the nutritional and sensory quality of the fruit by minimizing adverse biochemical alterations (such as the Maillard reaction). Furthermore, thin-layer empirical and semi-empirical mathematical models (e.g., Page, Henderson&Pabis, and Lewis) were fitted to the drying curves, demonstrating robust statistical validation through the coefficient of determination) R^2 ,(reduced chi-square) χ^2 ,(and root-mean-square error (RMSE). Fick's second law was successfully applied to determine the effective moisture diffusivity) D_{eff} (within the product matrix, proving this hybrid system to be a highly sustainable processing strategy for arid desert regions.

Keywords:

Indirect Solar Drying, Phase Change Materials (PCM), Paraffin Wax, Aluminum Shavings, Drying Kinetics, Orange Dehydration, Mathematical Modeling, Effective Moisture Diffusivity, El-Oued Region.

ملخص

تأتي هذه الدراسة في إطار التحول العالمي نحو تكنولوجيات الطاقة المتجددة، وتحديدًا لتطوير وتجويد أداء أنظمة التجفيف الشمسي غير المباشر عبر دمج تقنيات تخزين الطاقة الحرارية الكامنة لتجاوز مشكلة تقطع الإشعاع الشمسي. تم في هذا العمل إجراء دراسة تجريبية مقارنة ونمذجة رياضية لحركية تجفيف شرائح البرتقال (بسُمك 4 إلى 6 ملم ورطوبة ابتدائية تتراوح بين 85% و90%) في منطقة الوادي بالجنوب الشرقي الجزائري خلال صيف 2026. جرت المقارنة بين نموذجين للمجفف الشمسي غير المباشر ذي الحمل القسري: الأول يعتمد على لاقط شمسي مسطح تقليدي، بينما تم تدعيم اللاقط الثاني بدمج مادة مبتكرة ذات تغير طوري مركب تجمع بين شمع البارافين المصري وخرط الألومنيوم (PCM-ALSH) لرفع الموصلية الحرارية للمنظومة. وأظهرت النتائج التجريبية تفوقًا ملحوظًا للاقط المطور؛ حيث حقق ذروة حرارية أعلى وتأثيرًا مخمدًا (العطالة الحرارية) ساهم في استمرار تدفق الحرارة داخل حجرة التجفيف لعدة ساعات بعد غروب الشمس، مما أدى إلى تقليص زمن التجفيف الإجمالي بنسبة معتبرة والحفاظ على جودة المنتج الغذائي والحسية (تقليل تفاعل مايار وتلف الفيتامينات). كما تم تقييم وتوافق حركية التجفيف باستخدام النماذج الرياضية للطبقات الرقيقة) مثل نماذج Page و Henderson وLewis، وأثبتت المؤشرات الإحصائية R^2 وX^2 و RMSE مطابقة عالية للبيانات التجريبية، إلى جانب حساب معامل الانتشار الفعال للمجال المائي (D_{eff}) بالاعتماد على قانون فيك الثاني للانتشار.

الكلمات المفتاحية:

التجفيف الشمسي غير المباشر، المواد ذات التغير الطوري(PCM) ، شمع البارافين، خرط الألومنيوم، حركية التجفيف، شرائح البرتقال، النمذجة الرياضية، معامل الانتشار الفعال، منطقة الوادي.

List of Figures

FigI.1: Details of the solar dryer (a) schematic layout diagram of the dryer, (b) cross sectional view of the solar air heater (c) photograph of the dryer [1]. 5
FigI.2: The solar dryer: (a) Setup front view, (b) Setup back view [2]. 6
FigI.3: Experimental setup during experiment [3]. 7
FigI.4: Schematic view to description of the solar dryer Dry1[4]. 8
FigI.5:Schematic view to description of solar dryer with two compartment Dry2 [4]. 9
FigI.6: Schematic view to description of solar dryer with single compartment Dry [4]. 9
Fig I.7: Experimental setup of conventional and modified ISD [5]. 10
Fig I.8: Diagram of a solar drying system [6]. 11
FigI.9: Photograph of dryer [6]. 12
Fig.I.10: Construction and assembly process of the ISD prototype components [8]. 13
Fig II.1: Schematic Drying Mechanism [10] 17
Fig II.2: Principle of operation of solar dryer. 19
Fig II.3: Classification of solar dryers. 20
Fig II.4: Direct solar dryer 21
Fig II.5: indirect solar dryer 22
Fig II.6: Mixed-mode solar dryer. 22
Fig II.7: Solar drying systems with various heating systems [27] 23
Fig II.8: Curve showing the drying speed as a function of time [29]. 24
Fig II.9: Classification of Phase change Materials [33] 26
Fig. III .1: Construction and assembly process of the ISD prototype components. 33
Fig. III .2: Photograph and schematic design of the prototype ISDs experimental setup. 35
Fig. III .3: Diagram of the different steps of experimental protocol preparation. 37
Fig. III .4: Oranges slices weighed and distributed on trays of the ISD chamber. 38
Fig. III .5: Clear glass 38
Fig. III .6: flat panel collector 39
Fig. III .7: The fan used in the indirect solar dryer 39
Fig. III .8: Experimental setup of the drying chamber. 40
Fig. III .9: Drying product support. 40
Fig. III .10: The paraffin that was used in the thermal energy storage system 41
Fig III.11: Thermocouples Nickel-Chrome/Nickel-Aluminium 42
Fig. III .12: Location of thermocouples 42
Fig. III .13: Testo 440 anemometer + Testo 610 thermo-hygrometer 43

Fig. III .14: Lutron gm-500 digital scale, 500g x 0.1g, rs-232 43
Fig. III .15: Photograph of the 12-channel temperature recorder 44
Fig. III .16: Daily variation of ambient temperature (**Tamb**) and solar radiation (**Qrad**) during May 2026. 48
Fig. III .17: Temperature evolution over time for the collector with PCM and the conventional collector. 49
Fig. III .18: Comparison of the evolution of the collector temperature obtained by the PCM model and the conventional model during the day. 50
Fig. III .19 : Variation of ambient temperature (T_amb) over time (May 2026). 51
Fig. III .20: Hourly Variation of Solar Radiation (**Qrad**) and Temperature (T_7) - May 2026. 52
Fig. III .21: Experimental Temperature Evolution of a Solar Collector Integrated with Phase Change Material (PCM) vs. Conventional System 53
Fig III.22: Moisture content (w.b.) reduction of orange slices during the drying process over time. 54

List of Table

Tableau III. 1: Thermophysical properties of paraffin wax-aluminum composite PCM used in this study 36
Tableau III. 2: Prototype Instrumentation 41
Tableau III. 3: Different drying models.....46

Table of contents

Abstract .....

List of Figures .....

List of Table .....

Table of contents .....

General Introduction

Chapter I: Bibliographic study

I.1. Introduction 4

I.2. Bibliographic review of solar dryers 4

I.3. Conclusion: 14

Chapter II: General Aspects of Drying

II.1. Introduction 16

II.2. History of Drying 16

II.3. Definition drying 16

II.4. Drying Mechanism 17

II.5. Solar Dryers 17

II.6. Importance of solar dryer 18

II.7. Working Principle of Solar Dryers 18

II.8. Main factor of solar dryer 19

II.9. Classification of solar dryers 20

II.10. Advantages of food preservation by drying 23

II.11. Benefits of Food Preservation: 24

II .12. Stages of the Drying Process: 24

II.13. Drying efficiency: 25

II.14. Phase Change Materials 25

II.14.1. Definition of Phase Change Materials 25

II.14.2. Role of PCM in Solar Dryers: 26

II.14.3 Classification of Phase Change Materials (PCMs): 26

II.14. Conclusion 31

Chapter III: Experimental Approh and Modelling Data Analysis

III.1 Introduction 33

III .2. Materials and methods 33

III .3. Design and construction of the ISD prototype 34

III .3.1. Preparation of PCM tube 35

III .3.2. Drying product....38
III .3.3. Clear glass: 38
III .3.4. flat panel collector: 39
III .3.5. The fan:....39
III .3.6. Drying chamber:....40
III .3.7. The grid: 40
III.3.8. Paraffin (PCM): 41
III .4. Prototype Instrumentation 41
III.4.1 Measuring Temperature:....41
III.4.2Measuring humidity and air velocity:....42
III.4.3Lutron Gm-500 Digital Scale, 500g X 0.1g, Rs-232 :....43
III.4.4 Information Gathering and Handling: 43
III.5. Drying Kinetics Models....44
III.5.1Empirical Models 44
III.5.2 Diffusive Models 45
III.5.3Models based on coupled heat and mass transfer....45
III.5.4Determination of the Effective Diffusivity of Water 47
III.6. Observations and interpretations 48
General Conclusion 56
Bibliographical references 59

General Introduction

In light of the accelerating global shift toward renewable energy, solar energy is recognized as a strategic and reliable option with significant applications in ecological and industrial fields, particularly in solar drying technology, which offers effective engineering and economic solutions for preserving agricultural produce. Unlike traditional open-air sun drying, which degrades product quality and exposes crops to environmental contamination, developed solar systems provide a controlled sanitary environment that substantially reduces food waste. However, the intermittent nature of solar radiation during cloudy periods and after sunset poses a major obstacle to process continuity and stability. To address this constraint, the integration of thermal energy storage techniques, especially using Phase Change Materials (PCMs), has emerged as a pioneering technological solution that absorbs excess thermal energy as latent heat and releases it to sustain the drying process.

This academic thesis, conducted at Echahid Hamma Lakhdar University of El-Oued during the 2021/2022 academic year, presents a comprehensive laboratory study and comparative engineering analysis of two advanced Indirect Solar Dryer (ISD) prototypes operating under forced convection. The experimental runs were carried out under the severe, arid climatic conditions of the El-Oued region in southeastern Algeria during the summer of 2026. The first setup served as a baseline reference, utilizing a conventional flat-plate solar collector to supply the necessary thermal flux. Conversely, the solar collector of the second prototype was enhanced by integrating an innovative thermal composite material. This composite material marries the high latent heat capacity of paraffin wax with the superior thermal conductivity of aluminum shavings (PCM-ALSH), thereby overcoming the intrinsic thermal resistance of the base material and accelerating energy charging and discharging rates. To validate the dynamic efficiency of the drying mechanisms, orange fruits were selected as the testing medium due to their substantial national production surplus. Additionally, their high initial nexal moisture content (85-90%) provided an ideal evaluative baseline. The fruits were subjected to a uniform automated slicing process to achieve a precise thickness of 4 to 6 mm. This meticulous preparation ensured identical initial parameters for experimental verification and comparative analysis.

This thesis adopts a rigorously structured, chapter-based methodology to ensure academic coherence, beginning with a critical review of solar drying's historical evolution and modern thermal storage systems. The subsequent chapter elucidates the foundational scientific principles governing dehydration, focusing on heat and mass transfer phenomena while encompassing complex biochemical alterations such as the Maillard reaction. A dedicated chapter then delineates the empirical investigation, specifying the advanced instrumentation for monitoring solar radiation and temperature, and introduces a mathematical modeling approach

for drying kinetics utilizing thin-layer empirical curve-fitting. To ensure robust statistical validation, the derived models are evaluated against established metrics, specifically the coefficient of determination (R^2), reduced chi-square (chi^2), and root-mean-square error (RMSE). Additionally, Fick's second law is employed to calculate the effective moisture diffusivity (D_{eff}) within the product matrix, thereby integrating historical review, theoretical principles, and rigorous experimental validation to structure the research systematically.

In conclusion, Chapters III present a comprehensive discussion and comparative evaluation of the thermal performance achieved. The empirical evidence indicates that the collector incorporating custom rectangular tubes filled with the PCM-ALSH composite attained a superior thermal peak. Moreover, through latent heat discharge during solidification, it produced a pronounced thermal lag that prolonged effective drying activities for several hours beyond sunset. This favourable dynamic response functions as a thermal buffer, moderating abrupt temperature variations and enhancing moisture removal efficiency. Consequently, it offers a highly sustainable and scalable strategy for minimising post-harvest losses and fostering rural agricultural processing in arid desert regions.

Chapter I: Bibliographic study

I.1. Introduction

Solar drying is a diverse field that demands various techniques and specialized materials. Given the extensive research conducted in this area, this chapter reviews experimental studies on the solar drying of agricultural products, covering the technology's historical development, design configurations, equipment, and recent advancements. It examines different types of solar dryers and the range of agricultural products suitable for this process, while also assessing their benefits and limitations in terms of energy efficiency, cost-effectiveness, and environmental impact. In this context, heat storage technologies are essential for improving efficiency and reducing thermal losses. Notably, phase change materials (PCMs) can store and release significant amounts of thermal energy during solid-liquid phase transitions, making them valuable for smart buildings and renewable energy systems such as solar and wind power, where they help smooth energy demand peaks and enhance energy autonomy. However, key challenges remain, including high material costs, design complexity, and compatibility with existing systems. This study analyzes the advantages of PCMs, identifies the main technical obstacles, and explores future directions, offering useful insights for both researchers and professionals in the field.

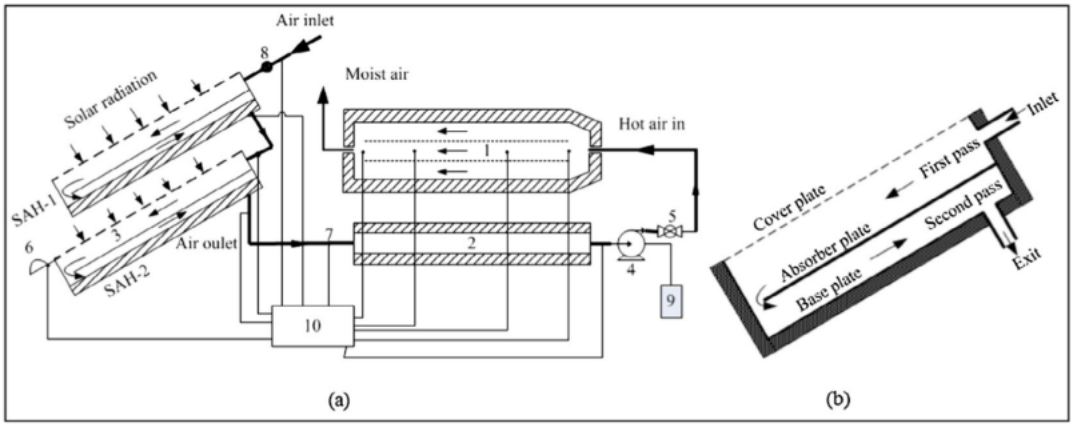
I.2. Bibliographic review of solar dryers

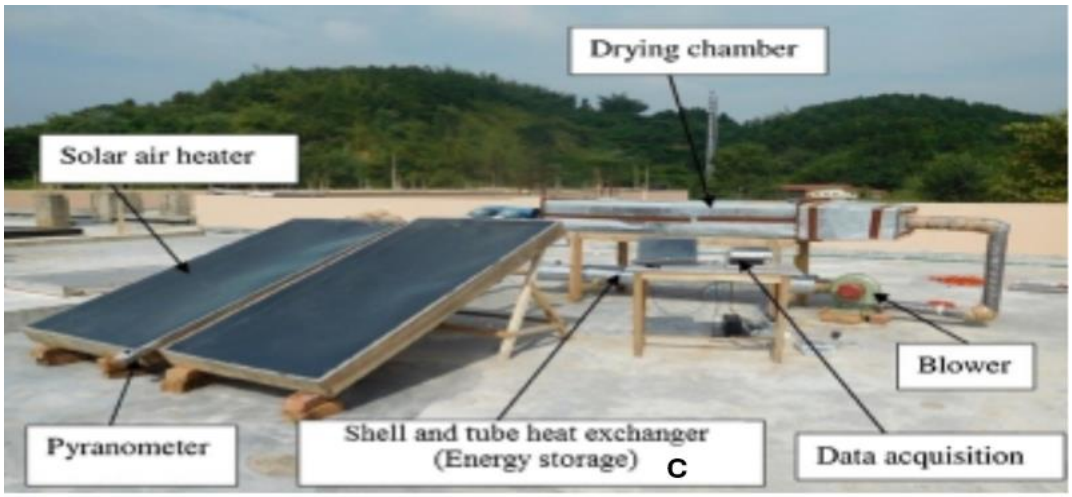
In 2017, D.K. Rabha, et al.[1]conducted a study presented the performance evaluation of a forced convection solar dryer integrated with a paraffin wax-based shell and tube latent heat storage unit. The system comprised two series-connected double-pass solar air heaters, a latent heat storage module, a blower, and a drying chamber. To assess its functionality, 20 kg of red chili with an initial moisture content of 73.5% (w.b.) was dried over four consecutive days, during which the drying air temperature ranged from 36 to 60 °C, and the dryer operated daily from 8:00 to 18:00. The final moisture content was reduced to 9.7% (w.b.). Energy and exergy analyses were conducted to evaluate each component’s performance. The first and second solar air heaters exhibited average energy efficiencies of 32.4% and 14.1%, and exergy efficiencies of 0.9% and 0.8%, respectively. The latent heat storage unit achieved energy and exergy efficiencies ranging from 43.6% to 49.8% and from 18.3% to 20.5%, respectively, while the drying chamber’s exergy efficiency varied between 24.6% and 98.1%, averaging 52.2%. The overall drying system efficiency was 10.8%, with a specific energy consumption of 6.8 kWh per kg of moisture removed. Notably, electrical energy consumption

accounted for only 0.7 kWh per kg of moisture, just 10.3% of the total specific energy. The latent heat storage played a crucial role by sustaining higher drying air temperatures beyond

the solar heater outlet after 14:30, enabling continued operation until 18:00, and reducing temperature fluctuations during cloudy periods. Compared to open sun drying, this hybrid system reduced drying time by 122.8%. Overall, the evaluated performance parameters confirmed the technical feasibility and effectiveness of the proposed integrated solar drying system. (see Fig.1).

(a) 1. Parallel flow tunnel dryer; 2. Shell and tube heat exchanger (energy storage); 3. Solar air heater; 4. Air blower; 5. Ball valve; 6. Pyranometer; 7. Thermocouple; 8. Flow meter;9 Energy meter; 10. Data acquisition system.





FigI.1: Details of the solar dryer (a) schematic layout diagram of the dryer, (b) cross sectional view of the solar air heater (c) photograph of the dryer [1].

Experimental investigation of an active direct and indirect solar dryer withsensible heat storage for camel meat drying in Saharan environment investigated by Wafa Braham Chaoucha,b et al.[2]investigationA novel solar dryer combining direct and indirect forced convection, integrated with a pebble-based sensible heat storage system, was developed and tested under the harsh climatic conditions of the Algerian Sahara. The system featured a direct

drying chamber placed above an indirect drying chamber, with one pebble bed located in a plenum beneath the direct chamber and another in a cavity under the solar collector. The heat storage unit improved the solar collector's thermal efficiency by 28% and maintained its performance for up to one hour after sunset, while the direct chamber's thermal efficiency increased by 11.8%. Drying experiments on unsalted camel meat were conducted in July and November, revealing faster drying kinetics in July due to higher temperatures. Among several mathematical models tested, the logarithmic model best described the drying behavior in July, and the Midilli–Kucuk model was most suitable for November. The average indirect drying efficiency over the diurnal period reached 18.34% in July and 15.52% in November, while direct drying efficiency averaged 10.35% and 7.88%, respectively. To preserve protein content, the usual salting pretreatment was omitted. Microbiological and physicochemical monitoring confirmed that the final quality of the dried meat met Algerian regulatory standards and was satisfactory overall, especially when compared to open-sun drying, which resulted in significantly lower hygienic and physicochemical quality.(see Fig.2).



FigI.2: The solar dryer: (a) Setup front view, (b) Setup back view [2].

Recently, Dheerandra Singh et al. [3]experimentally investigated an indirect-mode natural convection solar dryer integrated with a phase change material (PCM) for drying banana slices. The drying system comprised a solar collector containing paraffin wax as the PCM, and a drying chamber equipped with two evenly spaced trays. The paraffin wax stored latent and sensible heat, releasing it after sunset to maintain effective drying for an additional five hours. During the experiment conducted in April 2018 in Gorakhpur (Fig.3)., Uttar Pradesh, India, 400 g of banana slices were dried from an initial moisture content of 73.2% (wet basis) to 20%

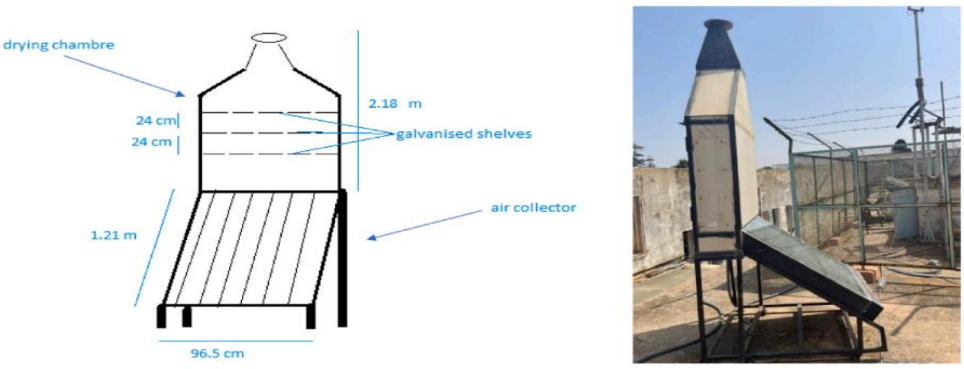
in 18 hours, comprising 13 hours of daytime operation and five hours of PCM-assisted drying. Fourteen thin-layer drying models, both empirical and non-empirical, were fitted to the experimental data using XL-Stat software for nonlinear regression analysis. Among these, the Modified Henderson and Pabis model best described the drying behavior of the banana slices. The average drying rates for the lower and upper trays were 0.1316 and 0.1310 kg of water per kg of dried product per hour, respectively, with the lower tray showing faster moisture reduction, as its moisture ratio dropped from 100% to 28%. The dryer achieved maximum and average efficiencies of 9.88% and 2.98%, respectively, while the collector reached maximum and average efficiencies of 85.46% and 66.32%, respectively. The findings demonstrated that an indirect solar dryer using paraffin wax was well-suited for drying bananas, as it significantly reduced drying time and could be extended to other agricultural crops. Solar energy remained an ideal low-temperature heat source for agricultural drying. The use of paraffin wax extended operation by five hours after sunset, enhancing overall performance and minimizing drying time. The Modified Henderson and Pabis model is recommended for characterizing the thin-layer drying of bananas in such systems. Overall, integrating thermal energy storage offers a promising solution for rural areas, and performance could be further improved by incorporating dehumidification before solar air heating or by using forced convection to optimize inlet airflow rates, thereby reducing drying time and increasing efficiency.



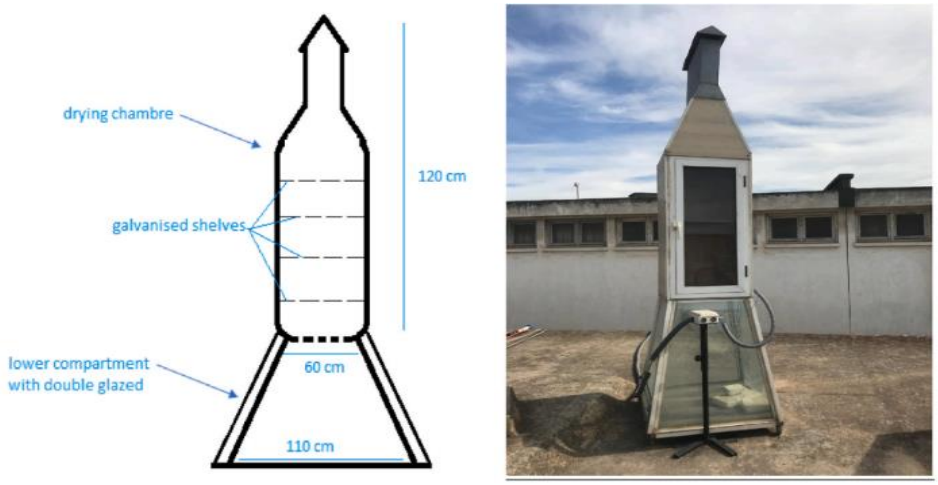
FigI.3: Experimental setup during experiment [3].

In 2022,H. Krabch , et al.[4]conducted investigated the drying kinetics and quality of orange slices using three indirect, naturally convected solar dryers, while a data acquisition

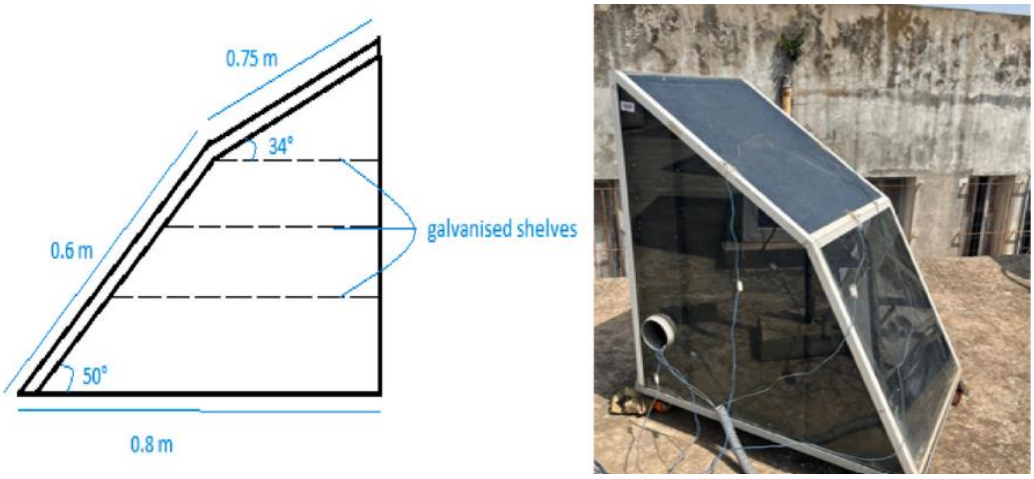
system monitored climatic variables such as temperature, relative humidity, and solar radiation to compare thermal performance. Experimental measurements conducted over several days in April and May revealed that the average outdoor temperature did not exceed 19.5 °C, whereas the average internal temperatures reached 40 °C in the third dryer (Dry3), 34 °C in the first (Dry1), and 28 °C in the second (Dry2). Outdoor relative humidity ranged between 60% and 85%, while inside the dryers, humidity varied from 5% to 35% for Dry3, 5% to 70% for Dry1, and 32% to 75% for Dry2. Under these conditions, orange slices lost 72% of their initial mass after 6 days in Dry3, compared to 15 days in Dry1 and 18 days in Dry2. Among the three prototypes, Dry3, featuring a single-compartment design with absorber walls, proved the most effective in terms of thermal performance and drying duration. It also had the lowest cost (750 USD), compared to 1,240 for Dry1 and 1,100 for Dry2, and was easier to construct without specialized labor. Dry1, with a conventional configuration of a solar air collector and drying chamber, achieved intermediate performance (average 34 °C, 37.5% humidity) and dried oranges in 15 days with a moisture diffusivity of 3.11×10^{-10} m²/s, but its cost was relatively high. Dry2, consisting of a lower double-glazed heating floor and an upper drying floor, showed lower performance (average 28 °C, 53.5% humidity), required 18 days to reach a 72.3% evaporation rate, and had a moisture diffusivity of 1.56×10^{-10} m²/s. Drying slowed considerably at night in Dry1 and Dry2 due to sharper temperature drops, which suggested the need for thermal storage. Notably, all three dryers achieved a reduction in orange slice weight from an initial 1005 g to approximately 273 g, thereby preserving nutritional quality. However, the final condition of oranges dried in Dry1 and Dry3 was superior to that in Dry2. With an average temperature of 40 °C and a low average humidity of 20%, Dry3 enabled complete drying in just 6 days and achieved an effective moisture diffusivity of 7.78×10^{-10} m²/s. Overall, Dry3 was the most beneficial and economically viable option, encouraged its adoption by local producers.(see Fig.4,5,6).



FigI.4: Schematic view to description of the solar dryer Dry1[4].



FigI.5:Schematic view to description of solar dryer with two compartment Dry2 [4].



FigI.6: Schematic view to description of solar dryer with single compartment Dry [4].

Acomparative experimental analysis of potato slice drying using a multiple PCM cascaded modified indirect solar dryer and conventional indirect solar dryer investigated by Panchal et al.[5]investigated the use of multiple phase change materials (M-PCMs), specifically Bheem paraffin (50–55 °C) and paraffin wax (60–62 °C), cascaded beneath the absorber plate of a solar air he (SAH) to enhance the performance of a conventional indirect solar dryer (ISD) for drying potato slices (Fig.7). Experiments were conducted simultaneously on conventional and modified ISD systems in Valsad, India, with an air velocity of 15 m/s. Two batches of potato slices (0.5 kg and 0.3 kg per tray) were tested. Results demonstrated that the modified ISD achieved faster drying times (2 hours less for the bottom tray and 1 hour less for the top tray in the first batch) and significantly higher drying percentages in the second batch (92.11% in the bottom tray and 54.35% in the top tray), representing increases of 269.92% and 227.41% over the conventional ISD, respectively. Over 12 hours, the modified ISD evaporated 1.13 kg

of water, whereas the conventional system evaporated 0.87 kg. Compared to the conventional ISD, the modified ISD achieved a 22.29% and 7.92% enhancement in SAH efficiency (excluding and including blower power, respectively), a 29.69% improvement in overall drying efficiency, and a 22.87% reduction in specific energy consumption. Additional findings included higher daily average temperature differences (14.46%) and relative humidity differences (40.19%) at the drying chamber, which indicated improved heat and moisture transfer. Overall, the integration of M-PCMs significantly enhanced drying performance during both sunshine and off-sunshine hours.



Fig I.7: Experimental setup of conventional and modified ISD [5].

In 2024, Kai Xu et al.[6]conducted a study on a solar drying kiln for wood, which integrated a phase-change heat storage and dehumidification system to address the high energy consumption and adverse environmental impact associated with conventional drying methods. Using simulation software (TRNSYS and MATLAB), the researchers modeled the system's temperature distribution and operating parameters over a one-year period. The results demonstrated strong consistency between simulated and measured temperatures, withan average relative error of 2.29%. The optimal operating conditions were identified as follows: a dehumidifier airflow rate of 1500 m^3/h, a solar panel inclination angle of 36°, and a control scheme in which the dehumidifier was deactivated when the drying room temperature reached 55 °C and reactivated when the temperature fell below 55 °C. As a result of the simulation and optimization, the average indoor temperature increased by 24.05%, system energy consumption decreased by approximately 56.23% (equivalent to 43,156.54 kWh annually), and CO_2

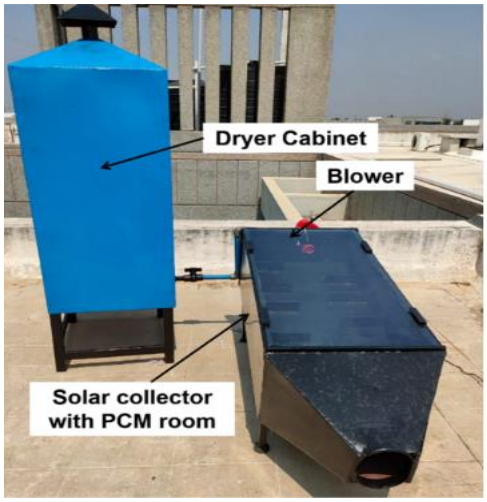
emissions were reduced by 3,312.22 kg. Taken together, these findings provide a practical pathway for enterprises to achieve tangible energy savings and emission reductions in wood drying processes (see Fig. 8).



Fig I.8: Diagram of a solar drying system [6].

In 2025, M.K. Murthi et al.[7]conductedStudy on an indirect where a crucial role in the food industry by enabling the preservation of various perishable products—such as cereals, vegetables, and fish—through effective moisture removal. In this study, an indirect-type cabinet solar dryer was constructed specifically for drying bitter gourd pieces. To improve the dryer's performance during the late evening hours, an inorganic salt, sodium thiosulfate pentahydrate ($Na_2S_2O_3 \cdot 5H_2O$), was incorporated into the collector area as a phase change material (PCM), an approach seldom discussed in the existing literature. The research evaluated key parameters, including moisture ratio, moisture reduction rate, inlet and outlet temperatures, and overall drying efficiency under two configurations: an indirect solar dryer without PCM (IDSD) and one with PCM (IDSD-PCM). The experiments-maintained a constant air mass flow rate of 0.07 kg/s over nine hours per experimental day. The results showed that integrating sodium thiosulfate pentahydrate significantly influenced the drying chamber temperature, especially during the late evening. Moreover, using PCM increased the daily moisture extraction from sliced bitter gourd by 2.8%, while system efficiency improved by 3.6% with the PCM-enhanced setup. The indirect solar dryer was purpose-built for dehydrating bitter gourd slices, with the

sodium thiosulfate pentahydrate PCM placed within the solar collection area. Trials lasting nine hours compared the IDSD and IDSD-PCM configurations. The inclusion of PCM raised the drying chamber's inlet temperatures for an additional hour beyond daylight hours. The moisture content of the bitter gourd pieces dropped from 92% to 7.6% using IDSD alone, whereas the PCM further reduced it to 4.8% by extending the dryer's operational period. Consequently, drying system efficiency increased from 20.8% to 24.4% due to the enhanced thermal storage of the system. Nevertheless, the system requires testing under varying climatic conditions to confirm its suitability for year-round use. Future research is recommended to include exergy and enviro-economic assessments of the IDSD-PCM system to further validate its reliability for prolonged operation. (see Fig.9).



FigI.9: Photograph of dryer [6].

Recently, MENECEUR et al.[8]experimentally evaluated two indirect solar dryer (ISD) prototypes in El-Oued, Algeria (July 2025) to address efficiency constraints caused by solar radiation fluctuations(see Fig.10).. The first prototype used a conventional solar collector, while the second incorporated square tubes filled with a composite phase change material composed of paraffin wax and aluminum shavings (PCM-ALSH). The results demonstrated that the PCM-ALSH-integrated dryer significantly outperformed the conventional system. Specifically, it achieved a maximum useful heat gain of 550 W (which was 12% higher), an average thermal efficiency of 52% (compared to 30%), and a maximum exergy efficiency of 7.5% (representing a 65% improvement). The PCM extended heat release for up to 8 hours after sunset and maintained drying chamber temperatures 1–8 °C above ambient conditions. Consequently, drying time was reduced from 32 to 26 hours (a 30% reduction). Overall, the PCM-ALSH composite proved to be an effective energy storage solution that enhanced efficiency, stabilized drying processes, and enabled sustainable agricultural processing.



Fig.I.10: Construction and assembly process of the ISD prototype components [8].

I.3. Conclusion:

In conclusion, the integration of phase change materials (PCMs) and sensible heat storage systems into solar drying technologies represents a significant advancement in the field of agricultural product preservation. As demonstrated throughout this bibliographic review, thermal energy storage not only enhances the thermal efficiency and reliability of solar dryers but also extends their operational hours beyond sunshine periods, reduces drying time, and improves the overall quality of dried products.

The studies reviewed confirm that PCM-based and hybrid storage systems contribute to more stable drying chamber temperatures, lower specific energy consumption, and reduced environmental impact. Notably, systems incorporating paraffin wax, composite PCMs, or cascaded multiple PCMs have shown substantial improvements in energy and exergy efficiencies, while sensible heat storage solutions, such as pebble beds, have proven effective in arid regions like the Algerian Sahara. These findings underscore the critical role of thermal storage in enabling more sustainable and cost-effective drying processes, particularly for off-grid and rural applications.

However, several challenges remain, including the high cost of PCM materials, design complexities, and the need for compatibility with existing dryer configurations. Future research should focus on developing low-cost, eco-friendly PCMs, optimizing heat exchanger designs, and integrating dehumidification or forced convection strategies to further enhance performance. Long-term field tests under diverse climatic conditions are also necessary to validate the techno-economic feasibility of these systems.

In summary, the use of thermal energy storage in solar dryers offers a promising pathway toward reducing post-harvest losses, lowering fossil fuel dependency, and advancing sustainable agricultural practices. Continued innovation and interdisciplinary collaboration will be essential to overcome current limitations and fully realize the potential of this technology for a more energy-efficient and environmentally friendly future.

Chapter II:General Aspects of Drying

II.1. Introduction

Solar drying has been acknowledged as an efficient and economical technique for preserving agricultural products. Conventional open-air sun drying presents several significant issues, including exposure to UV radiation, dust contamination, and the influence of external variables such as insects, animals, and pathogens. These constraints typically hinder compliance with international quality and sanitation standards. Sun drying is a conventional method, however laborious and prone to mould proliferation, especially during adverse weather conditions. Moreover, it requires substantial effort and subjects the products to environmental contaminants. To tackle these issues, more sophisticated solar drying techniques have been devised.[9] Solar dryers are categorised into three types: direct, indirect, and mixed mode. Moreover, solar dryers can be categorised according to their utilisation of forced or natural convection for airflow. This chapter introduces solar drying systems, their classifications, and the application of Phase Change Materials (PCM) as an energy storage solution to enhance drying efficiency and reliability.

II.2. History of Drying

The method of drying agricultural crops has been utilised globally for numerous centuries. Seeds, leaves, and fruits are often desiccated by placing them in direct sunshine for several days on a firm, level surface, protected from precipitation, rodents, and insects. The food is thereafter stored in diverse containers and warehouses after confirming it has attained an adequate level of dryness using tactile assessment, and is safeguarded from dew to avert rehydration. This method of drying crops and food is an effective and time-honoured approach for conserving food and preventing wastage due to the natural deterioration of perishable items, and it remains prevalent today.

II.3. Definition drying

Drying is a crucial process employed for both agricultural and commercial products. It is the method of removing moisture from objects. Drying reduces bacterial proliferation in goods, rendering it an advantageous technique for their long-term preservation. Drying serves as either a preservation method or a stage in the processing of specific materials. It is used in rural regions to dry agricultural products and meats, as well as in industries like as food and textiles. Biologists have determined that reducing the moisture content of food to between 10 and 20% successfully eradicates bacteria, fungi, and enzymes. The flavour and most of the nutritional value are preserved and enhanced. Dried things can be preserved for several months. Moreover,

a dehydrated food item weighs around one-sixth of its fresh counterpart. They necessitate no specialised storage apparatus and are convenient to transport.[9]

II.4. Drying Mechanism

To desiccate a substance, it is adequate to circulate adequately heated and arid air. A transfer of heat and moisture transpires between this air and the damp product. The heated air conveys heat to the product, resulting in a partial pressure of water on its surface that exceeds the partial pressure of water in the drying air. This pressure differential induces the migration of material from the solid's surface to the drying air. Consequently, two critical elements must be managed throughout drying processes:

- Heat transmission to supply the latent heat necessary for vaporisation;

The transfer of water or water vapour through the moist product to facilitate its extraction from manufacture. [10]

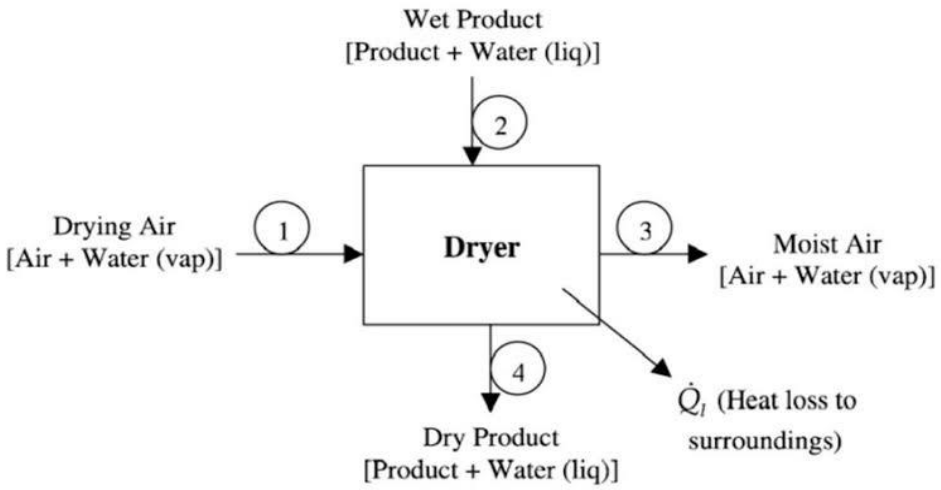


Fig II.1: Schematic Drying Mechanism [10]

II.5. Solar Dryers

Dryers can be classified in various ways, depending on the perspective adopted. A potential criterion is the product's texture, which affects its handling and interaction with drying air or hot surfaces. A different classification may be founded on the drying mechanism itself. In boiling dryers, the product is boiled to a temperature at which the vapour pressure of its moisture matches the ambient total pressure. In convective dryers, the product is positioned within an airflow that possesses a vapour pressure lower than that at the surface of the product. Solar dryers are generally classified into three categories: • Direct solar dryers, in which items are subjected directly to sunshine.

- Indirect solar dryers, in which items are not exposed to direct sunshine.
- Mixed solar dryers that integrate both techniques.

The drying rate is a crucial determinant in selecting the suitable drying technique. Relative humidity substantially affects the solar drying process. Other significant design considerations are the type of absorber, building materials, angle of inclination, and the transparent cover orientated towards the sun. [11].

II.6. Importance of solar dryer

Drying is a crucial post-harvest procedure in agricultural productivity. It has been utilised since antiquity to preserve agricultural produce. The procedure of extracting moisture from a product is recognised and can be executed [12]. This practice is seen essential for the preservation of agricultural products, particularly in areas with ample sunlight. It provides a sustainable and environmentally friendly alternative to traditional drying technologies that frequently depend on fossil fuels. Solar dryers leverage solar energy to diminish post-harvest losses, boost product quality, and prolong shelf life by efficiently extracting moisture that fosters microbial proliferation. Moreover, sunlight drying reduces contamination from dust, insects, and environmental pollutants, hence enhancing hygiene relative to open sun drying. From an economic standpoint, solar drying reduces energy expenses and enhances the revenue of farmers and small-scale enterprises by facilitating value addition and market development. [13].

II.7. Working Principle of Solar Dryers

Solar dryers employ solar energy to extract moisture from objects, typically food items, using regulated heating and airflow. This approach provides a sanitary and effective substitute for conventional sun drying. Solar dryers function by transforming sunlight into thermal energy, which is subsequently utilised to remove moisture from the items. The fundamental elements comprise:

- **Solar Collector:** Absorbs solar radiation and transforms it into thermal energy. The collector generally has a black surface designed to absorb sunlight effectively.
- **Drying Chamber:** A confined area designated for the desiccation of items. The heated air from the solar collector is channelled into this chamber.
- **Airflow System:** Enables the circulation of heated air within the drying chamber, effectively removing moisture evaporated from the items.

Raising the air temperature reduces its relative humidity, hence augmenting its ability to absorb moisture from the items. This procedure persists until the requisite moisture content is attained.[14]

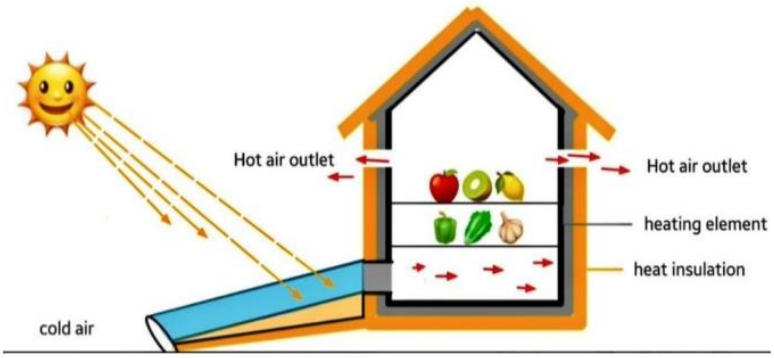


Fig II.2: Principle of operation of solar dryer.

II.8. Main factor of solar dryer

Solar drying systems are often categorised into two types: direct and indirect. They may also be classified as either active or passive. The efficacy of food dehydration in these systems is predominantly determined by three interconnected factors: temperature, airflow rate, and humidity. Despite differing viewpoints on ideal drying temperatures, the majority of studies concur on a range of 35°C to 82°C, with 43.5°C to 60°C being the most frequently employed.[15].

A. Solar Radiation Intensity

The quantity of solar energy available directly affects the drying rate. Elevated sun radiation results in greater temperatures within the drier, facilitating moisture evaporation from the product. Nonetheless, variations caused by meteorological circumstances can impact consistency.

B. Drying Air Temperature

By raising the vapour pressure difference between the moisture in the product and the surrounding air, higher air temperatures speed up the drying process. Depending on the substance being dried, ideal drying temperatures usually fall between 35.5°C and 70°C [16].

C. Airflow Rate and Velocity

Sufficient circulation eliminates the damp air from the drying chamber, preserving a gradient that encourages the product to continuously lose moisture. To guarantee effective drying without physically harming fragile materials, air velocities between 1-2 m/s are frequently advised [17,15].

D. Relative Humidity of Drying Air

The drying air's ability to absorb moisture from the product is improved by lower relative humidity. It is crucial to design dryers that can preheat or dehumidify incoming air in humid locations since high ambient humidity might slow down the drying process [18, 14].

E. Initial Moisture Content of the Product

Higher initial moisture content products need more energy and longer drying times. Designing an efficient drying process requires an understanding of the moisture properties of the particular product.

F. Dryer Design and Type

Drying efficiency is influenced by the solar dryer's configuration, whether it is direct, indirect, or mixed-mode. For example, indirect dryers can provide better regulated drying conditions, shielding goods from contamination and direct sunlight [19].

G. Geographical and Climatic Conditions

The performance of solar drying is greatly influenced by the local climate, which includes typical temperatures, humidity levels, and solar insolation. sun drying applications work best in areas with high sun insolation and low product humidity.

II.9. Classification of solar dryers

Passive dryers (natural convection) and active dryers (forced convection) are the two basic types of solar dryers. Depending on how solar radiation energy reaches the product to be dried, three families of solar dryers—direct solar dryers, natural indirect and hybrid dryers, and mixed dryers—are successful in each category.[20]

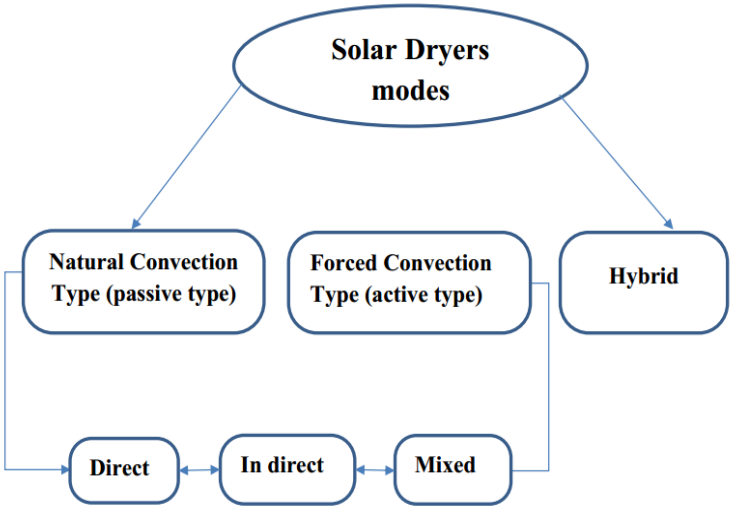


Fig II.3: Classification of solar dryers.

A. Natural Convection Type

In the natural kind, the product can dehydrate without the need for an outside source of heat. Solar dryers of the natural convection type might be direct, indirect, or mixed mode [21][19].

- **Direct Solar Dryer**

In direct solar dryers, the product is simply dehydrated by being exposed to sunshine. This kind of solar dryer has a black-painted heat-absorbing plate that can gather sunlight, absorb it, and turn it into heat. Direct placement of the product to be dried occurs on the absorber plate. To improve thermal efficiency, this dryer could incorporate vents and glass lid covers [22].

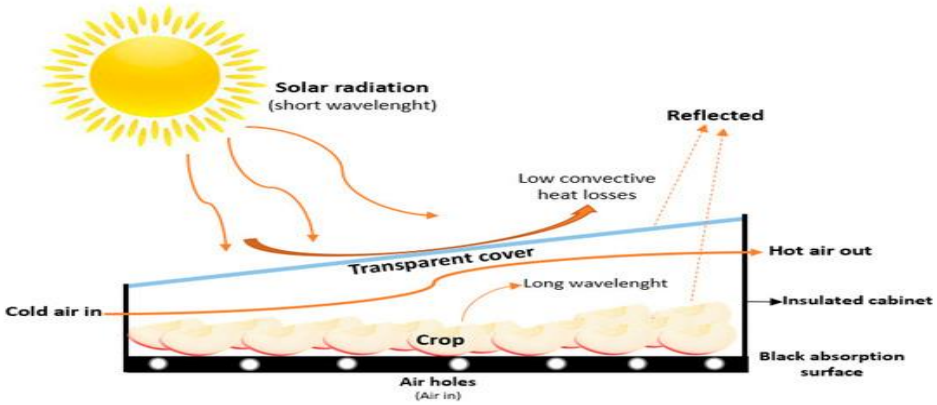


Fig II.4: Direct solar dryer

- **Indirect Solar Dryer**

By shielding the items from light rather than exposing them to direct sun radiation, indirect solar dryers assist maintain the nutritious value of the products. A solar collector and a drying chamber are the two primary parts of these dryers (Fig. II.5) [23]. In order to maximise solar energy absorption, the solar collector-which is often placed independently and attached to the drying chamber during operation-is slanted. It is made out of an absorbing surface that is frequently painted black to improve heat absorption and a transparent glass cover. The solar collector heats the air before directing it into the drying chamber. In this process, moisture is transported from the product to the air and heat is transferred from the heated air to the product [24][17].

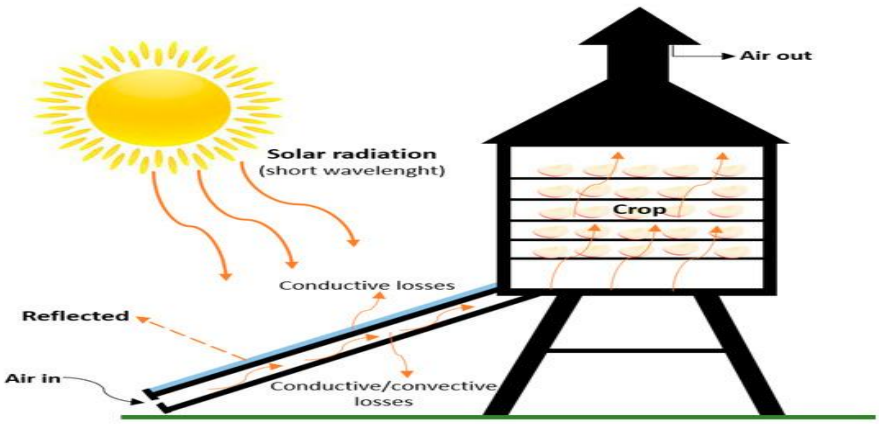


Fig II.5: indirect solar dryer

- **Mixed Mode Dryer**

Indirect and direct solar dryers are combined to create the mixed-mode solar drier. The heat required for the drying process is provided by the combined action of the solar intensity incident on the product to be dried and the air preheated in the solar collector. Figure II.6 is a diagram of a mixed-mode solar dryer. The heat required for the drying process is produced by the combined action of the sun intensity incident on the product to be dried and the air preheated in the solar collector. [25].

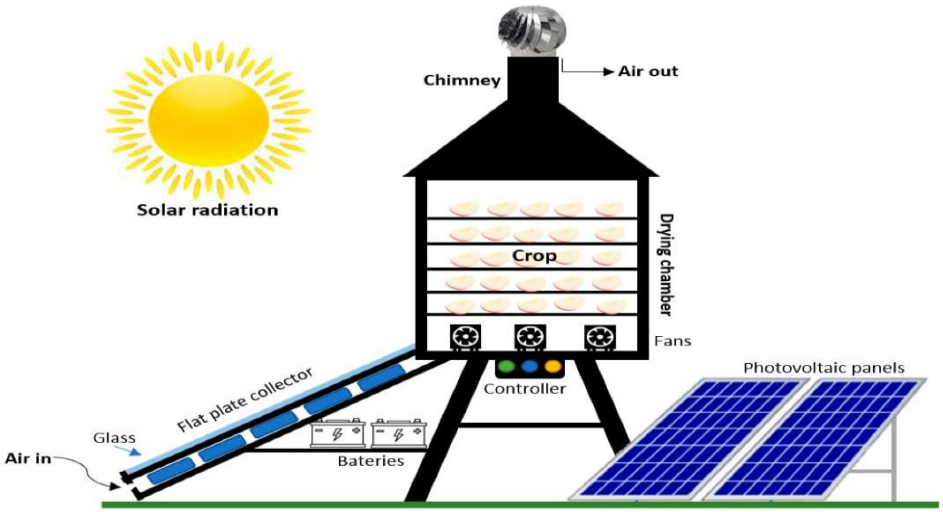


Fig II.6: Mixed-mode solar dryer.

B. Forced Convection Type

These dryers operate and are similar to natural convection dryers, but they have an extra fan or blower that continuously blasts hot air over the objects to be dried, making drying quicker and more effective. These dryers are capable of drying a variety of agricultural products due to their relative thermodynamic competence [26].

- **Hybrid solar dryers**

To guarantee a high degree of air heating or to offer ventilation, these dryers use an additional energy source (fuel, electricity, wood, etc.) in addition to solar energy. In this situation, solar energy is frequently utilised to warm the air. These more costly systems are often saved for commercial or large-scale applications where the final product's flow rate and quality may be affected by the weather. The drying techniques that are most frequently employed in industry are:

– Hot air drying or "traditional" drying
– Superheated steam drying;
– Heat pump drying;
– Hot chamber drying;
– Vacuum drying;

The last two drying processes are used especially for wood drying [27].

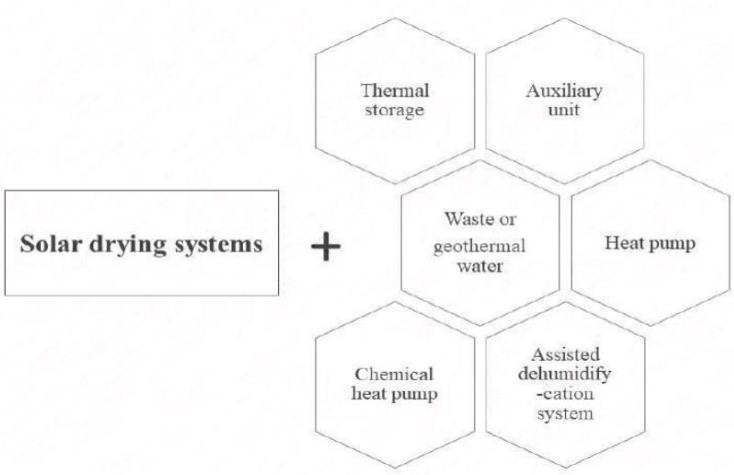


Fig II.7: Solar drying systems with various heating systems [27].

II.10. Advantages of food preservation by drying

Foods including fruits, vegetables, seafood, meat, and aromatic herbs and mushrooms can all be preserved through drying. The growth of bacteria, mould, and yeast that cause spoiling and decay can be stopped by removing water and concentrating sugars, especially in the case of fruits. When compared to alternative preservation techniques, drying offers a number of benefits. You don't need a big refrigerator to keep frozen goods.

Minerals preserve flavours that are unaffected by the addition of oil, vinegar, salt, sugar, alcohol, or fermentation, and are not diluted in water. A significant amount of vitamins are

preserved, with the exception of vitamins C and B, which are both partially and totally destroyed. decreases food's weight and volume: When storage space is scarce, dried goods are helpful because they require a lot less room than fresh ones [28].

II.11. Benefits of Food Preservation:

- Solar drying is cheaper than other methods of food preservation, such as canning and freezing, and does not require the addition of preservatives.
- Reduces the cost of storage, packaging, and transportation because drying reduces the volume and mass of dried materials as they lose most of their moisture.
- Makes out-of-season food more affordable.
- Increases farmers' income by preserving surplus crops from spoilage in the absence of cold storage facilities

II .12. Stages of the Drying Process:

Curves are the most effective way to explain a product's drying properties. The product moisture content (ns) as a function of time or the drying speed (dt/dns) as a function of time are two of the best illustrations of the stages of the drying process. Krischer has suggested an alternative method of expressing the moisture content (ns) and drying speed (dt/dns), which is depicted in (Fig. II.8) [29].

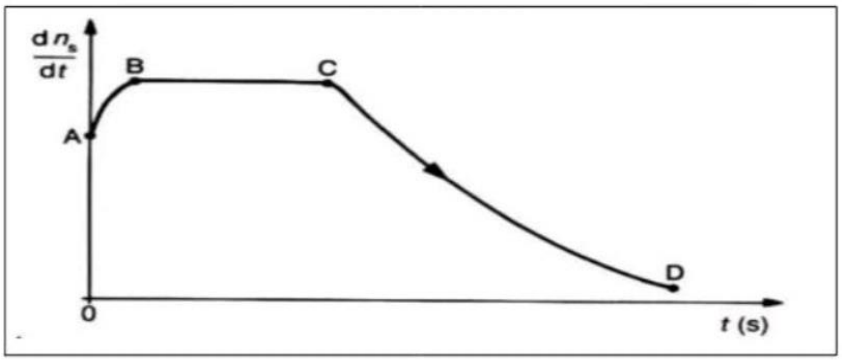


Fig II.8: Curve showing the drying speed as a function of time [29].

These three types of representation highlight the existence of several stages in the drying process. Not all of them are observablesystematically, we distinguish from them:

- **Stage One: The Increasing Stage (AB)**

Typically, when a thin layer of water exists as a vented volume on a surface, the removal of this layer during the drying process mirrors the evaporation of water from the surface of a water-filled container.

The duration necessary to finish the initial phase is directly contingent upon the thickness of the water layer on the material's surface. This duration is brief. During this phase, humidity fluctuates gradually, while the temperature ascends until it nears the dry-bulb temperature threshold. This phase is brief, and it remains ambiguous if the product is cumbersome or of substantial volume.[29]

- **Second Stage: Constant Drying (BC) Stage**

During this phase, the drying rate stays uniform for the majority of materials, with moisture migrating to the surface in liquid state due to capillary forces. This establishes equilibrium between the film diffusion process and the transference of internal moisture to the surface. The temperature is consistent across the material, as convection facilitates the evaporation of water to the surface.

- **Third Stage: Decreasing Drying (CD) Stage**

During this stage, the drying rate decreases, making it difficult for water to evaporate from the product. This

decrease is explained by:

- The disappearance of free water from the surface of the material.
- The movement and diffusion of water within the material to be dried until it reaches the outer surface [31].

II.13. Drying efficiency:

- **Aglomerular efficiency:**

The mass yield is substantially influenced by the characteristics and dimensions of the product, moisture content, temperature, and air velocity surrounding the product.

- **Energy efficiency:**

In the drying process, two quantities characterize the energy consumed:

- Average energy consumption is the amount of energy required to evaporate 1 kg of water from the product.
- Energy consumption ratio

II.14. Phase Change Materials

II.14.1. Definition of Phase Change Materials

Materials for Phase Change Phase Change Materials (PCMs) are materials that release energy during the solidification heat transition and absorb it during the melting heat transition

from solid to liquid. Throughout the fusion and solidification processes, phase transition heat exhibits a high thermal density and little temperature variation. A solid that gains energy by melting when heated is known as a phase transition material. The melting temperature might vary within a small range or remain constant. As the liquid solidifies, the stored energy is recovered.

II.14.2. Role of PCM in Solar Dryers:

Phase Change Materials (PCMs) play a crucial role in enhancing the performance and efficiency of solar dryers. Here's how:

A. Thermal Energy Storage

During periods of high solar radiation, Phase Change Material absorbs excess heat. They store thermal energy as latent heat when they melt. The PCM then solidifies and releases the stored heat when sunlight decreases (for example, in the evening or on cloudy days), maintaining the drying temperature.

B. Continuous Drying Process

Phase Change Materials (PCMs) help the drying process in the absence of solar radiation by stabilising the dryer's internal temperature. This leads to faster and more reliable drying, which improves the quality of the final product.

C. Temperature Regulation

Phase Change Materials shield heat-sensitive items from overheating and deterioration by reducing temperature swings within the drying chamber.

D. Energy Efficiency

By minimising heat loss and efficiently using stored energy, they enhance the system's overall energy efficiency, which can lower drying time and expense.

II.14.3 Classification of Phase Change Materials (PCMs):

A large number of phase change materials (organic, inorganic, and eutectic) are available in all required temperature ranges. [30].

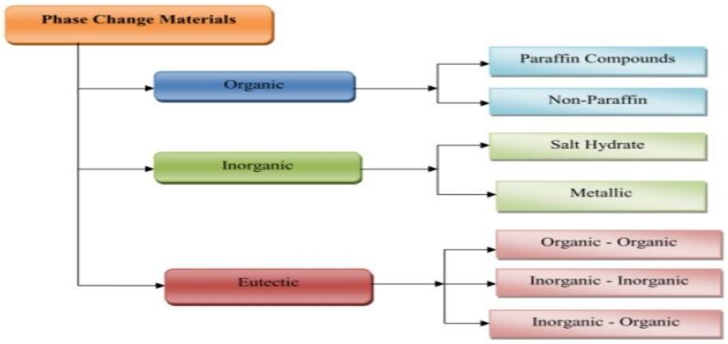


Fig II.9: Classification of Phase change Materials [33]

- **Organic materials**

Paraffins and fatty acids make up the bulk of organic phase change materials that have been investigated. After several heat cycles, paraffins show outstanding chemical and thermal stability. Stearic, lauric, myristic, capric, and palmitic acids are the fatty acids that have been extensively researched. Most of the fatty acids used as phase transition materials are of industrial quality. [31].

- **Inorganic materials**

This group is mainly composed of salts or hydrated salts and metals.

- **Hydrated salts**

The general formula for a hydrated salt is AB•nH2O, where n is the number of water molecules and AB is the anhydrous salt's formula. Phase transition materials have been made from a range of hydrated salts. Hydrated salts have high thermal conductivity and a large latent heat of fusion per unit volume. Additionally, they have very little volume during the transitional stage. They work well with polymers and have low corrosivity. CaCl2•6H2O is the hydrated salt that is most frequently used. One

- **Eutectic**

A mixture of two or more compounds, either organic, inorganic, or a combination of both, is called a eutectic phase change material (PCM). In contrast to pure chemicals, several researchers have shown a great deal of interest in novel eutectic-type phase change materials within the last ten years. Fatty acids and salt hydrates make up the majority of organic and inorganic eutectics that have been classified as phase change materials (PCMs).

❖ HYBRID SOLAR PV/THERMAL SYSTEM

With diverse capacity for producing clean electricity and a declining reliance on conventional energy, solar system accreditation has increased dramatically in recent years. A drawback of the photovoltaic system is that when the temperature rises to a point where it affects the solar cells, the effectiveness of the PV panel decreases and occasionally even the cells degrade. The efficiency of solar cells can be maintained by a variety of methods. One such method is a cooling system that lowers the high temperature of the solar cells by using air as a heat transfer medium through ducts positioned beneath the plate and in contact with the PV panels. Water, which has a high thermal capacity, is used as a medium in another method. Using an absorber plate with embedded tubes that absorb the high temperature of the PV cells and keep it within an acceptable range, the cooling mechanism in this system targets the PV panel

from the back. This makes it possible to generate thermal energy from the heat produced by the PV system and electrical energy with great efficiency. Since the PV/thermal system's overall efficiency reflects its inherent worth, numerous researchers have created a variety of methods to boost the system's efficiency while optimising the output power. Consequently, a novel method was employed to enhance the PV/thermal system's performance, which is exemplified by the addition of PCMs to the solar collectors. As seen in Fig. 5, these PCMs have a significant advantage in terms of heat absorption and release. When the temperature rises, they collect heat from the PV panel, which is then released through the fins at night. They can be used to cool solar cells when the temperature rises because of this benefit. The efficiency of the PV panel is increased by using PCMs, which enable the solar cells to function at a temperature that is almost constant. After the PV panels are positioned in rectangular metal fins to disperse the heat buildup, a fatty acid is utilised as the PCM to cool the panels. The PCM's (fatty acid) limited heat conductivity helps to increase PV efficiency. [32].

- **Concept of a Hybrid System and How It Works**

When solar power is insufficient (for example, on cloudy days or at night), a hybrid system can store the electricity in batteries and use the grid or generator as backup sources. The system's hybrid inverter controls the energy flow between the panels, batteries, and the grid or generator, ensuring that the house or building has a steady supply of electricity even during blackouts.

- **Auxiliary Power Sources Used**

The following are commonly utilised in hybrid systems: When the sun or batteries aren't producing enough electricity, on-grid electricity can be produced as a backup using diesel or gas generators. Some systems combine solar and wind energy to improve production consistency throughout the day and night. [33].

❖ **Key Advantages**

- **Continuous Power Supply:** Provides continuous power to the batteries and auxiliary source (grid or generator) even during power outages or adverse wind and sun conditions.
- **Reduced Electricity Bill:** Primarily relies on solar power, reducing consumption from the grid or generator and protecting against price hikes
- **Renewable Energy with Flexibility:** Combines the advantages of grid-connected (to-grid) and off-grid systems, allowing connection to the grid and partial reliance on generators when needed.

❖ **Key Disadvantages**

- **High Initial Costs:** Requires a solar system + batteries + hybrid inverter + often a generator or grid connection, which initially raises the market cost.
- **Design and Maintenance Complexity:** Requires additional equipment and more precise control in managing power between sources.
- **Nutritional Changes that Occur After Drying:**The drying process must be carried out in a way that preserves product quality without significant changes at the end of the process. Since bitter products differ medically from the original product in several ways, most agricultural and food products are affected by drying.
- **Physical and Mechanical Changes:**The process of removing water from the product leads to its self-decomposition, and the shape of the final dried product differs from the original shape. The phenomena of solution translocation to the surface, fat translocation, cracking, and shrinkage negatively affect product quality. [34].

❖ **Biochemical Modification**

– High t

– emperatures for prolonged periods cause harmful changes in food.

- **Main Changes:**

– **The Maillard:** reaction is a non-enzymatic biological reaction resulting from the interaction between proteins: and carbohydrates, producing brown products. However, these reactions lead to nutritional loss. Protein aggregation: limits the product's ability to recover after drying Enzymatic reactions: have a coloring effect on the product. To reduce this effect, the enzyme process must be slowed down by pretreatment, such as boiling or lowering the drying temperature.

  - Destruction of vitamins
  - Oxidation (damage) of fats

- **Loss of aroma and color**

The water in the product to be dried is removed by the presence of other volatile substances in the product, such as flavorings in agricultural and food products. The drying effect on the color of the product is less in a drying system with a low temperature and forced agitation compared to the original product.

- **Sensory quality:**

It is a combination of the different design senses that you get through the selection and consumption of the product. Products are evaluated by visual aspects, such as color, size, shape,

uniformity, and lack of deformation. This aspect is very important in assessing product quality. The sense of taste is limited to sweetness, sourness, saltiness, and bitterness. Flavor involves the senses of taste, smell, and texture. Flavor is often lost in dried products due to the loss of insecticidal substances, as they undergo the same process in which water vapor is transferred from the product to the outside. Similarly, chemical reactions cause a loss of flavor.

- **Nutritional quality**

This includes chemical parameters such as sugar content, acidity, vitamin C, corbic acid, beta-carotene content, and acidity before and after drying. Vitamin C is affected by high temperatures, resulting in decreased quality. [35]

II.14. Conclusion

This chapter presented a comprehensive overview of the drying process and its importance in preserving agricultural products, with particular emphasis on solar drying technologies and their applications in orange dehydration. The fundamental principles of drying, including heat and mass transfer mechanisms, drying stages, and the main parameters affecting drying efficiency, were discussed. Different types of solar dryers, such as direct, indirect, mixed-mode, and hybrid systems, were reviewed, highlighting their advantages in improving product quality and reducing dependence on conventional energy sources.

The integration of thermal energy storage materials, particularly Phase Change Materials (PCMs), was identified as an effective approach for enhancing solar dryer performance. These materials contribute to maintaining a stable drying temperature, extending the drying period beyond solar availability, and improving overall energy efficiency. Furthermore, hybrid solar systems combining photovoltaic and thermal technologies offer promising solutions for achieving continuous and sustainable drying operations.

Although drying provides significant benefits in terms of extending shelf life, reducing weight and storage requirements, and limiting microbial deterioration, it may also cause undesirable changes in nutritional and sensory properties, such as vitamin degradation, color alteration, and aroma loss. Therefore, optimizing drying conditions, including temperature, airflow rate, and humidity, remains essential to obtaining high-quality dried products.

Overall, the knowledge developed in this chapter provides the necessary theoretical foundation for modeling the drying kinetics of oranges and evaluating the performance of solar-hybrid drying systems integrated with thermal energy storage. The following chapter will focus on the mathematical modeling and experimental investigation of the drying process to determine the optimal operating conditions for efficient orange dehydration.

Chapter III: ExperimentalApproh and Modelling Data Analysis

III.1 Introduction

Solar drying has become a valuable process in Algeria, thanks to the abundant solar radiation available throughout the country. Its primary purpose is to preserve agricultural products for use at any time of the year. This chapter focuses on investigating the solar drying behavior of oranges, using an indirect solar dryer that was pre-designed and constructed for this study. In addition, mathematical models based on experimental data are employed to describe the drying process.

III .2. Materials and methods

An indirect sun dryer (ISD) using forced convection was implemented at the Research Unit in Renewable Energies for Arid Zones (UDERZA) in El Oued, Algeria (latitude 33.3639° N, longitude 6.8671° E).

designed, constructed, and assembled for experimental evaluation. Two advanced ISD prototypes, derived from and refined based on prior research, were meticulously fabricated at the UDERZA workshop using locally sourced, premium materials. Figure 1 depicts the several stages involved in the manufacturing and assembly of the ISD prototype components. [36].



Fig. III .1: Construction and assembly process of the ISD prototype components.

III .3. Design and construction of the ISD prototype

This experiment included the design, fabrication, and testing of two indirect sun dryers (ISDs) under the climatic conditions of El Oued City, southeastern Algeria. The solar dryers were fabricated using locally obtained, economical wood. One dryer functioned as a benchmark.

while the other was enhanced by integrating a phase change material (PCM), namely paraffin wax combined with aluminum shavings. Each solar dryer included two primary components: an air solar collector, designed to optimize the temperature of the airflow, and a drying chamber where the produce was situated. The solar collector was fabricated with dimensions of 175 cm in length, 75 cm in breadth, and 10 cm in thickness.

The external walls and base of the collector were insulated with a polyethylene foam layer, painted in black to capture solar radiation, and further strengthened with thermal wool insulation and wood to reduce heat loss. Conventional solar air collectors use a black-painted iron plate to maximize heat absorption. Conversely, the collector integrated with PCM contained paraffin wax combined with aluminum shavings, which were positioned in rectangular iron molds.

A 5 mm thick glass cover was affixed atop both collectors to facilitate unidirectional airflow and enhance heat retention throughout the drying process. Ambient air was introduced via a port situated below the center of the collector, using a fan to propel external air through certain input apertures, so enhancing airflow and expediting the drying process. The exit port was situated at the upper section of the solar collector and linked to the drying chamber. Silicone was used to guarantee an impermeable barrier between the collection and the drying chamber. The drying chamber was fabricated from 18 mm thick compressed wood panels, including a wall composed of three layers: two external hardwood p lates with a 4 cm thick polyethylene foam layer in between (refer to Fig. 1a and b). This layer functioned as insulation, exhibiting a thermal conductivity of around 0.039 (W/mK). This design aimed to preserve hot air inside the chamber and reduce thermal losses. Warm air was admitted via an aperture at the base of the chamber, while moist air was evacuated through a chimney-like hole at the apex. The sun drying chamber dimensions were 0.75 m × 0.65 m × 0.60 m, resulting in a total volume of 0.229 m^3. It had three plastic mesh trays particularly engineered to enhance airflow and optimize the drying process. The experiments were conducted on sunny days in May 2026, with both ISD prototypes-oriented southward to maximize solar radiation capture during the experimental duration. All elements of the prototype ISDs are shown in Fig. 2.

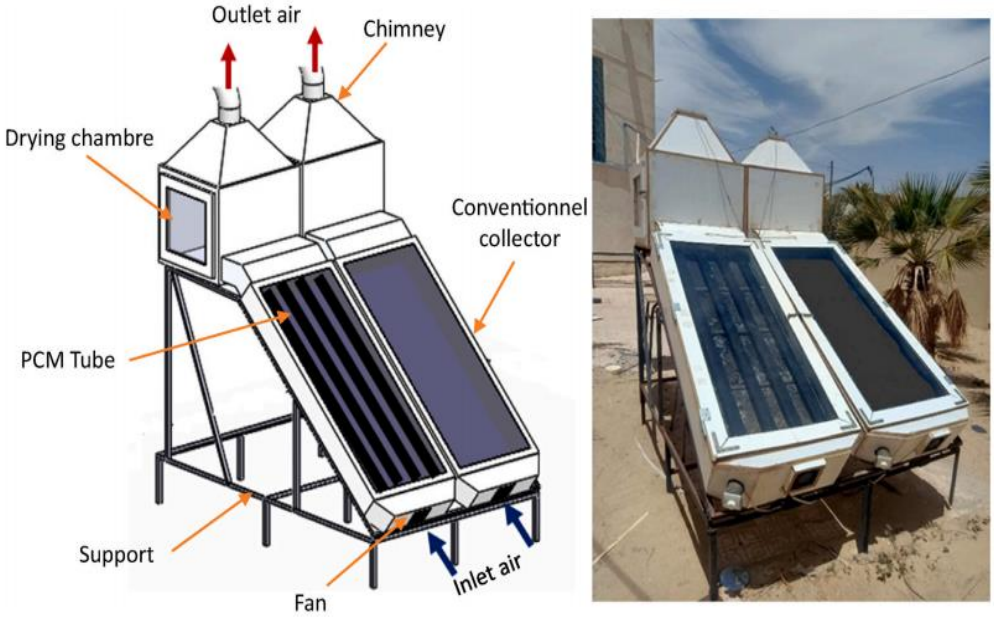


Fig. III .2: Photograph and schematic design of the prototype ISDs experimental setup.

III .3.1. Preparation of PCM tube

An Egyptian paraffin wax, commercially available and possessing a phase transition temperature range of 56-58 ◦C, was chosen as the phase change material (PCM) for its appropriateness to the specified thermal working conditions. [37] The thermophysical characteristics of the paraffin wax-aluminum composite phase change material used in this study are shown in Table 1. Furthermore, paraffin wax is extensively used in solar thermal applications.

Storage applications because to its comparatively high latent heat, exceptional chemical stability, non-corrosive properties, economical nature, and safe handling attributes. Nonetheless, its practical constraint is inadequate thermal conductivity, which may hinder heat transmission during melting and solidification. To address this restriction, aluminum shavings were integrated into the paraffin matrix to create a thermally enhanced composite phase change material (PCM-ALSH). In the experimental setting, 9.5 kg of paraffin wax was measured using a high-precision digital balance, thereafter heated, and evenly combined with 0.56 kilogram of aluminum shavings. The homogenous slurry was thereafter dispersed uniformly into four custom-fabricated rectangular tubes. Each tube is 150 cm in length, with cross-sectional dimensions of 6 cm by 4 cm and a wall thickness of 1.8 mm. These tubes were meticulously constructed for the experiment, with one end hermetically sealed by welding and the other end fitted with a screw cap to firmly shut the system post-filling. This structural design guaranteed mechanical stability during the filling process and the ensuing heat cycle activities

[1].Geometric estimates indicate that each tube has an interior volume of roughly 520.56 cm^3, resulting in a total PCM storage capacity of 3.6 L per tube, with each tube carrying 2.3-2.5 kg of the composite PCM mixture.

Upon introducing the paraffin-aluminum combination into the tube, it was meticulously stirred to eradicate any air pockets and to guarantee uniform dispersion of the aluminum particles inside the paraffin. The filled tubes were thereafter placed on a firm platform and let to cool naturally at ambient temperature. Upon transitioning to its solid state, the paraffin accurately conformed to the internal geometry of the tubular cage. The technique was executed four more times to provide a total of four iron rods packed with the paraffin-aluminum combination, which were then painted black to improve solar absorption. The whole preparation procedure lasted for almost three and a half hours. Figure 3 delineates the successive stages of the experimental process.

Throughout the filling procedure, the thermocouples were strategically placed at the specified measurement locations inside the PCM-ALSH mixture to guarantee precise temperature monitoring.

The primary aim of incorporating aluminum shavings into paraffin wax was to create a sophisticated thermal energy storage composite that synergistically merges the substantial latent heat capacity of paraffin with the improved thermal conductivity of aluminum. Paraffin

Tableau III. 1:Thermophysical properties of paraffin wax-aluminum composite PCM used inthis study [2]

properties	Value	Unit	Measurement Standard
Melting temperature	56-58	℃	ASTM D87/D3418
Latent heat of fusion	190	KJ/Kg	DSC analysis
Thermal conductivity: Solid / Liquid	0.24/0.22	W/mK	ASTM E1225
Specific heat capacity: Solid/ Liquid	2000/2150	KJ/KgK	DSC analysis

Density (Solid/Liquid phase)	910/790	Kg/m^3	ASTM D792
Aluminium shaving proportion	25	V %	

Wax, a frequently used phase change material (PCM), has significant benefits, such as increased energy storage density, chemical stability, and economic viability.

Nonetheless, its practical applicability is limited by its intrinsically poor thermal conductivity, which hinders effective heat transmission during

Phase transition. To alleviate this constraint, thermally conductive aluminum shavings were evenly included into the paraffin matrix. This composite construction enhances internal heat dispersion, consequently expediting energy charging and discharging rates.

Thus, the paraffin-aluminum composite offers a feasible and cost-effective method for improving the thermal efficiency of sun drying systems while maintaining the energy storage capacity and dependability of traditional phase change materials. The PCM-ALSH preparation technique was executed in accordance with recognized procedures for composite PCM preparation and encapsulation as documented in the literature [38]Table 1 presents a summary of the standardized testing methodologies used to evaluate the thermophysical properties of PCM .

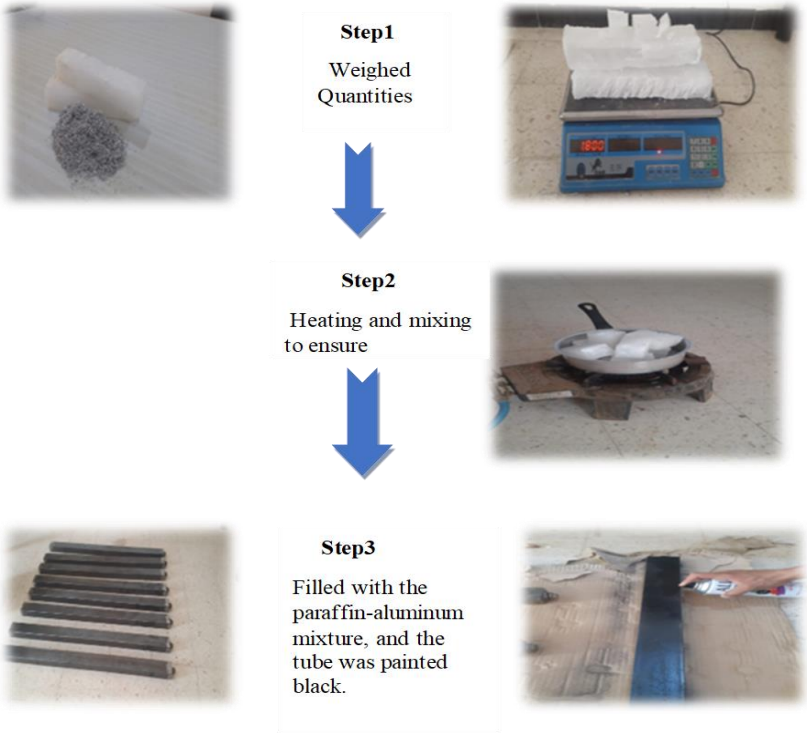


Fig. III .3: Diagram of the different steps of experimental protocol preparation.

III .3.2. Drying product

This research used orange fruit as a drying material to assess the efficacy of the solar dryer. Oranges were chosen because of a recent excess in national production this year, along with its designation as one of The 10 most eaten fruits in Algeria. Moreover, their elevated moisture content, often ranging from 85% to 90%, coupled with a fibrous, water-laden structure, renders them particularly suited for assessing moisture removal efficacy and generating shelf-stable dry goods customised to local market demands

Prior to dehydration, the oranges were uniformly cut into pieces with a thickness ranging from 4 to 6 mm using a calibrated manual slicer. The consistency of thickness was confirmed using a digital calliper to provide similar drying conditions for all samples. Samples weighing 285 ± 5 g were uniformly allocated on each

tray inside the drying chamber (refer to Fig. 4) to guarantee uniform testing conditions. [39].



Fig. III .4: Oranges slices weighed and distributed on trays of the ISD chamber.

III .3.3. Clear glass:

It is a transparent, robust, lightweight substance with safety attributes, thermal insulation, and UV resistance. Due to its attributes that facilitate sunlight penetration, withstand weather conditions, and provide efficient and reliable drying, it is an excellent choice for solar dryers.



Fig. III .5: Clear glass

III .3.4. flat panel collector:

The flat panel collector in the indirect solar dryer is used to heat the air using solar energy without directly exposing the product to sunlight.The absorber panel absorbs solar radiation and then transfers the heat to the air passing through the ducts, which is then directed to the drying chamber to remove moisture from the agricultural products.This system helps improve drying quality and reduce drying time while preserving the nutritional value of the product and reducing energy consumption.S[40].



Fig. III .6: flat panel collector

III .3.5. The fan:

The fan in an indirect sun drier is crucial for maintaining airflow and ensuring efficient drying. It eradicates humid air, promotes even heat and moisture distribution, and prevents the formation of stagnant air pockets. The fan significantly enhances drying efficiency by facilitating moisture evacuation and reducing the likelihood of condensation.



Fig. III .7: The fan used in the indirect solar dryer

III .3.6. Drying chamber:

The chamber is constructed from a variety of wood species and is well-insulated on all sides. It measures 0.75 m × 0.65 m × 0.60 m and is attached to the solar panel by a conduit that lets air flow through perforations to disperse it across the dried goods.



Fig. III .8: Experimental setup of the drying chamber.

III .3.7. The grid:

as shown in Fig. (III-6), is a support for the product that has holes for water drainage and is fastened by four balanced rods so that we may weigh the object without removing it. The toughness and corrosion resistance of this grid are its defining characteristics.



Fig. III .9: Drying product support.

The grid: is a support on which the product is placed, with holes for water drainage, secured by four balanced rods to allow us to weigh the product without removing it, see Fig. III-8. This grid is characterized by its hardness and resistance to rust.

III.3.8. Paraffin (PCM):

Paraffin, as a phase-change material that retains thermal energy during periods of intense solar radiation, is used in indirect solar dryers. As solar radiation diminishes, it solidifies, releasing the accumulated heat and maintaining a consistent temperature inside the dryer. This creates a controlled drying environment, enhances efficiency, and prolongs the drying duration.



Fig. III .10: The paraffin that was used in the thermal energy storage system

III .4. Prototype Instrumentation

A number of operational factors were tested and tracked in order to enhance the indirect solar dryer prototype's performance. The following is a list of the equipment and tools used for measurement and data collection:

Tableau III.2: Prototype Instrumentation

1- K-type nickel-chrome/nickel-aluminum thermocouples
2- Testo Model 440 anemometer
3- Keithley 2701 data acquisition system
4- BTM-4208SD: 12 channel temperature recorder + SD card data recorder
5- EKO and EPPLY type pyranometers
6- KERN PCB 3500-2 type balance and KERN ABT 220-4M balance

III.4.1 Measuring Temperature:

K-type nickel-chrome/nickel-aluminum thermocouples are used to measure temperatures. These thermocouples have an accuracy of 0.1°C and can monitor temperatures up to 750°C (see Fig III.10)

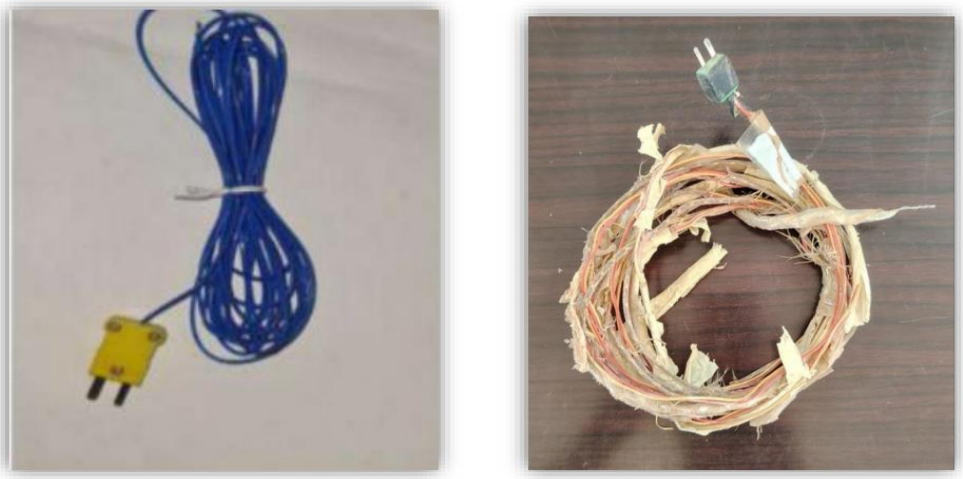


Fig III.11: Thermocouples Nickel-Chrome/Nickel-Aluminium

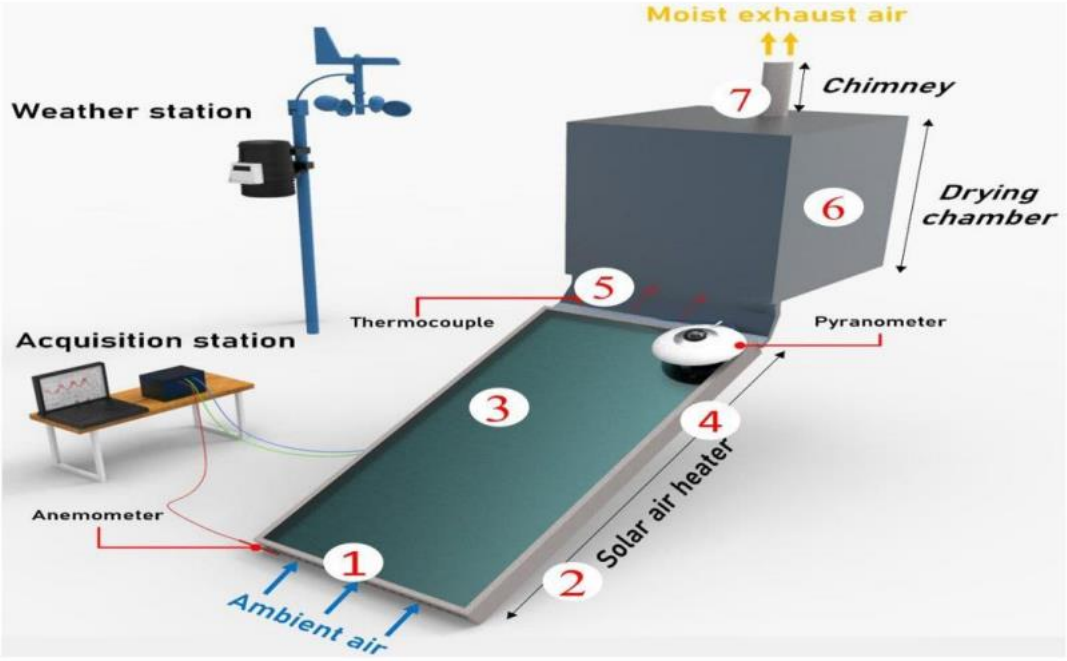


Fig. III .12: Location of thermocouples

III.4.2Measuring humidity and air velocity:

A Testo Model 440 anemometer is used to monitor the drying air velocity at the greenhouse-style solar dryer's outlet. The probe of the Testo 610 thermo-hygrometer is also used to detect relative humidity.



Fig. III .13: Testo 440 anemometer + Testo 610 thermo-hygrometer

III.4.3Lutron Gm-500 Digital Scale, 500g X 0.1g, Rs-232 :

This is a measuring instrument used to track the mass during drying (FigIII.14):



Fig. III .14: Lutron gm-500 digital scale, 500g x 0.1g, rs-232

III.4.4 Information Gathering and Handling:

The BTM-4208SD is a versatile A 12-channel temperature recorder that is linked to 12 thermocouples is part of the data collection and processing system. Data is collected and recorded using this technique (see Figure III.14).



Fig. III .15: Photograph of the 12-channel temperature recorder

III.5. Drying Kinetics Models

It is essential to derive a distinctive drying equation of the form M = f(t) that delineates the variation of reduced water content over time for the purpose of modeling drying curves. The drying kinetics curves are represented by empirical or semi-empirical equations that correlate water content with time, including constants obtained from experimental drying data. There are three sorts of drying models: those based on coupled heat and mass transfer, diffusive models, and empirical models. [41].

III.5.1Empirical Models

These models are based on trials and are therefore tailored to the product and the experimental settings used. Consequently, the application of these models is restricted. This empirical method is thus of limited use since it relies on the product specifications and the experimental parameters of the drying process.

- Wang Singh's Empirical Model (1978)

This empirical model was used to delineate the drying features of the utilized product, as per the equation:

$$MR = \frac{M - M_e}{M_o - M_e} = 1 + at + bt^2 \quad \text{(III.1)}$$

With constants a and b for drying. [42].

III.5.2Diffusive Models

The primary equation, most often used to characterize the thin-film drying process, resembles Newton's law of cooling. [43].It employs a single drying constant (k).

The equation proposed by Lewis (1921) has the following generic form:

$$\frac{dM}{dt} = -k(M - Me) \quad \text{(III.2)}$$

Assuming that the water content M is only a function of time, the solution to this equation, after integration, yields:

$$\text{MR} = \frac{M-Me}{Mo-Me} = \exp(-kt) \quad \text{(III.3)}$$

Here, k represents a drying constant influenced by temperature, absolute humidity, and the velocity of the drying air.

This type is well-suited for drying many items, including malt, bananas, peppers, and cassava [44].

III.5.3Models based on coupled heat and mass transfer

Page (1949), [48] provided a model for the drying of maize kernels, expressed in the following form:

$$\text{MR} = \frac{M-Me}{Mo-Me} = \exp(-kt^n) \text{(III.4)}$$

Ket and n are drying constants influenced by air temperature, absolute humidity, drying air velocity, [45].and the characteristics of the product.

This model is also adept in simulating the drying of agricultural items such potatoes, bananas, pistachios, and sugarcane.

The Henderson and Pabis (1961) model is likewise derived from Fick's second equation.

$$\text{MR} = \frac{M-Me}{Mo-Me} = A\exp(-Kt) \quad \text{(III.5)}$$

A and k represent the drying constants.

The logarithmic model employs an equation structured as follows:

$$\text{MR} = \frac{M-Me}{Mo-Me} = a\exp(-Kt) + c \qquad \text{(III.6)}$$

Where k, a, and c are drying constants dependent upon air temperature and velocity [46].

The following table compiles some drying kinetics models:

Tableau III. 3: Different drying models

Model Name	Model Equation	References
Henderson et Pabis	MR = a exp(-kt)	[50]
Wang et Singh	MR=1+at+bt²	[43]
Page	MR= exp(-kt^n)	[48]
Page modifiée	MR= exp(-(kt)^n)	[51]
Lewis	MR= exp(-kt)	[44] [52]
Parabolic	MR= a + bt + ct²	[51]
Logarithmic	MR = a exp(-kt) + c	[52]
Two-term exponential	MR = a exp(-kt) + (1-a) exp(-kat)	[53]
Verma	MR = a exp(-kt) + (1-a) exp(-gt)	[54]
Midilli-Kucuk	MR = aexp(-kt^n)+ bt	[55]

Among the ten models presented by the authors, as shown in Table III, the most appropriate model will be selected. Regression analysis was conducted using Origin Pro 8.0. The coefficient (R^2) was a primary criterion for selecting the optimal model to characterize the drying curves. The fit quality was evaluated using many statistical metrics, including R^2, reduced chi-square (χ^2), and root mean square error (RMSE). The below formula may be used to get these coefficients.

$$R^2 = 1 - \frac{\sum_{i=1}^{N}(MRexp,i - MRpre,i)^2}{\sum_{i=1}^{N}(MRexp - MRexp,i)^2} \text{(III.10)}$$

$$X^2 = \frac{\sum_{i=1}^{N}(MRexp,i - MRpre,i)^2}{N-n} \text{(III.11)}$$

$$\text{RMSN} = \sqrt{\frac{1}{N}\sum_{I=1}^{N}(MRpre,i - MRexp,i)^2} \text{(III.12)}$$

with

$$MRexp = \frac{\sum_{I=1}^{N} MRexp,i}{N} \text{(III.13)}$$

Where MRexp and MRpré denote the water content seen in the experiment and that predicted by the model, respectively. Statistical and correlation analyses, together with regression approaches, are extensively used in predicting the drying behavior of diverse agricultural crops. Linear and nonlinear regression models are crucial for delineating links between variables, particularly when authors have not demonstrated empirical connections.

III.5.4Determination of the Effective Diffusivity of Water

The mass transfer rate by pure diffusion is directly proportional to the concentration gradient of water content, in conjunction with the effective diffusion coefficient. Consequently, identifying this coefficient is crucial for accurately characterizing mass transfer in accordance with the analogous Fick's law, represented by the equation [56]

$$\frac{\partial \mathrm{MR}}{\partial \mathrm{t}} = \nabla[\mathrm{D_{eff}} \nabla \mathrm{MR}] \qquad \text{(III.14)}$$

Assuming the constancy of Deff, it is feasible to derive:

$$\frac{\partial \mathrm{MR}}{\partial \mathrm{t}} = \mathrm{D_{eff}} \nabla^2 \mathrm{M} \qquad \text{(III. 15)}$$

The dried product slice may be seen as a uniform plate exposed to a non-stationary gradual regime with a consistent starting distribution and uniform concentrations at the surface. Assuming the matrix is an infinite, undeformable plate (with no shrinkage or expansion), exhibiting a uniform initial moisture distribution, minimal external resistance, and constant diffusivity, the analytical solution of Fick's second law was formulated by Crank [57]

$$\mathrm{MR}=\frac{8}{\pi^2}\sum_{n=0}^{\infty}\frac{1}{(2n+1)^2}\exp(-(2n+1)^2\pi^2\mathrm{D_{eff}}t/4L^2) \text{ (III.16)}$$

Where: Defft represents the effective diffusivity (in m³/s), t is the time (in s), L signifies half the thickness of the slice (in m), and n is a positive integer.

For an adequately extended processing duration, all words in the subsequent sequence (n≥1) were deemed insignificant in comparison to the first term. Consequently, equation (III.17) may be represented as follows:

$$\mathrm{MR} = \frac{8}{\pi^2}\exp(-\pi D_{eff} t/4L^2) \text{ (III.17)}$$

The equation (III.18) may be restructured and articulated as follows:

$$\mathrm{Ln\ (MR)} = \mathrm{Ln}\left(\frac{8}{\pi^2}\right) - \pi^2 \mathrm{D_{eff}} t + 4L^2 \text{(III.18)}$$

Experimental drying data results are expressed as In (MR) in relation to rehydration time across various temperatures. The effective diffusivity is determined as follows:

$$\text{Slope (k)} = -\frac{\pi^2 D_{eff}}{4L^2} \quad \text{(III.19)}$$

III.6. Observations and interpretations

Finally, we will present the experimental results of this work, conducted in May 2026 at the Higher School of Desert Agriculture in El Oued, where the results will be presented in graphical form. These findings relate to two aspects: - The temperature changes at the absorber over a period of 10 hours, from 8:00 AM to 6:00 PM.

Evolution of the mass of paraffin dried in each drying chamber over the course of a day.

The variations in the mass of paraffin placed in each drying chamber were monitored for 17 hours, from 8:00 AM to 6:00 PM.

❖ **Results and Discussion**

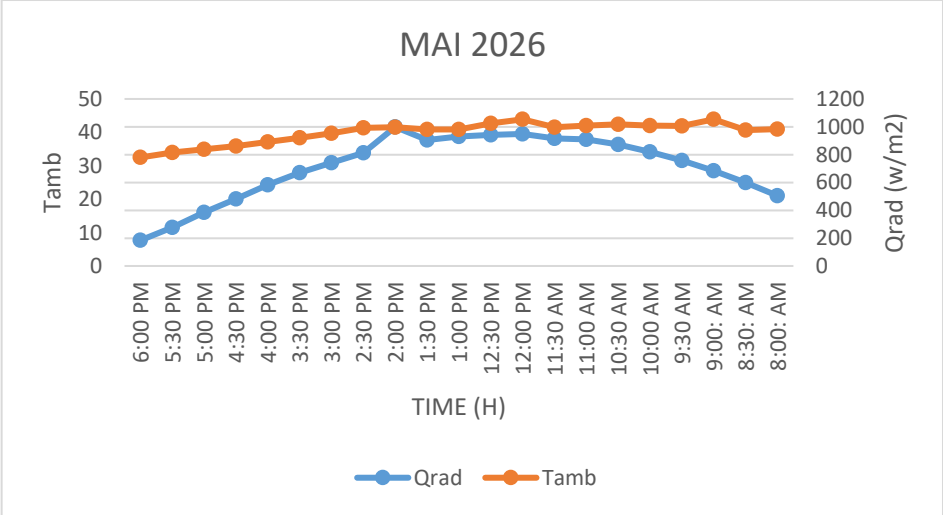


Fig. III .16: Daily variation of ambient temperature (T_{amb}) and solar radiation (Q_{rad}) during May 2026.

Fig.III.16 present the daily variation ofthe profiles of solar irradiance (Q_{rad}) and ambient temperature (T_{amb}) for May 2026, which must be interpreted from right to left due to the chart's reverse-chronological x-axis. Chronologically, Q_{rad} rises steadily from 500 W/m^2 at 8:00 AM to a midday plateau, ultimately peaking at approximately 1000 W/m^2 at 2:00 PM before sharply declining. Conversely, T_{amb} starts at an exceptionally high 41°C in the morning, reaches its maximum peak of roughly 44°C early at 12:00 PM, and steadily declines after 2:30 PM to a minimum of 32.5°C by 6:00 PM. This unusual behavior exhibits an inverted phase lag where the temperature peak precedes the irradiance peak, a phenomenon highly characteristic of extreme arid desert environments or localized microclimatic heating near the sensor.

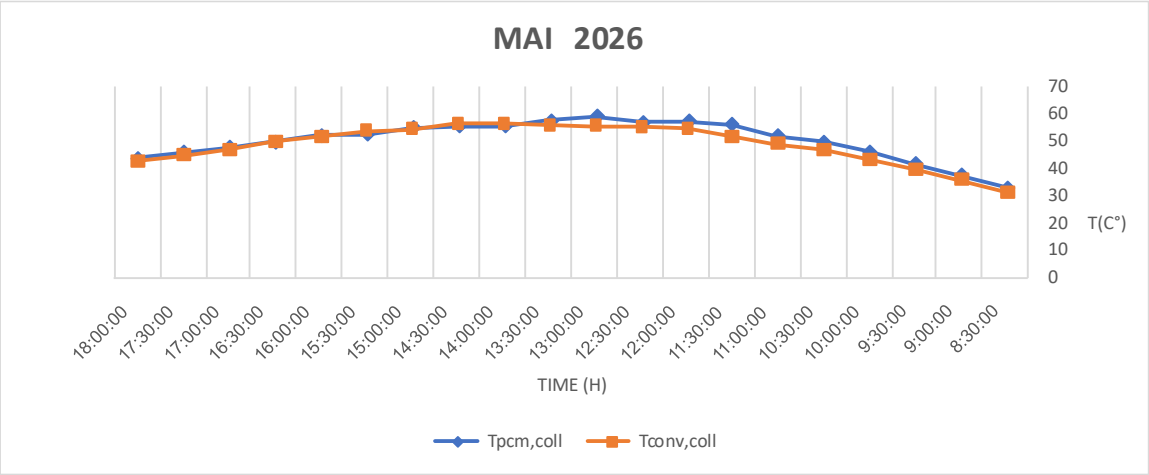


Fig. III .17: Temperature evolution over time for the collector with PCM and the conventional collector.

The figure (III.17) shows the temperature variation of the collector throughout the day for two configurations: a collector equipped with a phase change material (PCM) (blue curve: $T_{pcm,col}$) and a conventional collector without PCM (orange curve: $T_{conv,col}$).

The two curves follow a similar thermal evolution throughout the day. The temperature gradually increases from the first hours of measurement (around 8:00 AM), due to the increase in solar radiation received by the collector. The temperature then reaches a maximum around midday (between 12:30 PM and 1:30 PM), with a value close to 55–56 °C for the collector with PCM, while the conventional collector reaches a slightly lower temperature of approximately 52–53 °C. The presence of the PCM allows for a higher temperature to be maintained during periods of high solar irradiance thanks to its capacity to absorb and store thermal energy during the phase change. Thus, the PCM acts as a thermal regulator by limiting rapid temperature variations and maintaining a more stable collector temperature. After the solar maximum, both temperatures gradually decrease from the afternoon onward. However, the collector with the PCM maintains a slightly higher temperature than the conventional collector until the end of the studied period (around 6:00 PM). This difference demonstrates that the PCM gradually releases the stored heat, thereby improving the system's thermal inertia.

Compared to the conventional collector, the integration of the PCM therefore results in better thermal regulation, an increase in the collector's usable temperature, and more efficient storage of thermal energy during periods of reduced solar radiation

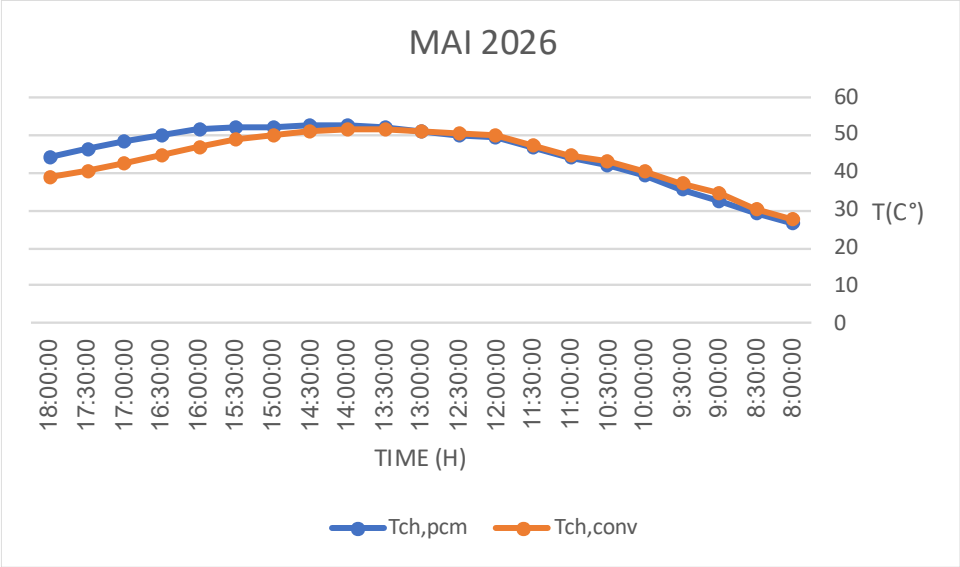


Fig. III .18: Comparison of the evolution of the collector temperature obtained by the PCM model and the conventional model during the day.

Figure III.18 illustrates the variation of collector temperature as a function of time for two cases: the collector integrated with a phase change material (PCM) model ($T_{ch,pcm}$, blue curve) and the conventional collector model ($T_{ch,conv}$, orange curve).

It can be observed that both curves exhibit a similar daily trend. The temperature increases progressively from 08:00 h, reaching a maximum value around 14:00–14:30 h, before decreasing gradually towards the evening. The peak temperature is approximately 52–53 °C for both configurations. A closer examination reveals that the collector temperature predicted by the PCM model is slightly higher than that of the conventional model during the morning period (08:00–13:00 h). The maximum difference remains limited, generally not exceeding 1-2 °C. Around midday, the two curves converge and become nearly identical, indicating similar thermal behavior under maximum solar irradiation. During the afternoon (14:30-18:00 h), the conventional model maintains temperatures marginally higher than those obtained with the PCM model. This behavior suggests that the thermal storage and release processes associated with the PCM contribute to moderating temperature fluctuations, resulting in a smoother thermal response. Overall, the difference between the two curves remains relatively small throughout the day, demonstrating that both models predict comparable collector temperatures. However, the PCM model provides a slightly more stable thermal profile by absorbing and releasing heat progressively, thereby reducing abrupt temperature variations and improving thermal regulation of the collector.

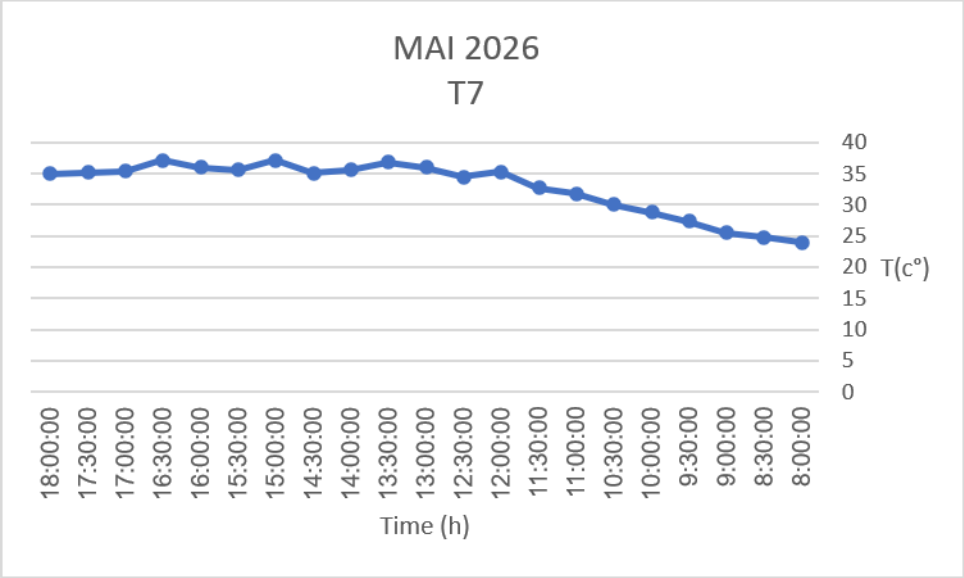


Fig. III .19 : Variation of ambient temperature (T_amb) over time (May 2026).

The figure shows the evolution of temperature as a function of time during the day for the month of May 2026 at Tamb.

The temperature profile exhibits three distinct phases: an initial heating phase during the morning, a stabilization phase around midday and early afternoon, and a gradual cooling phase toward the evening.

During the early hours of the day, from 08:00 to approximately 12:00, the temperature increases steadily from about 24 °C to nearly 35 °C. This rise is attributed to the increasing intensity of solar radiation reaching the collector surface. As the sun climbs higher in the sky, more solar energy is absorbed, causing a progressive increase in the collector temperature. The slope of the curve during this period indicates an efficient thermal response of the system to solar heating. Between 12:00 and 17:00, the temperature remains relatively high and stable, fluctuating within a narrow range of approximately 35-37 °C. The maximum temperature, close to 37 °C, is reached around 13:00-16:30. This plateau-like behavior suggests that the thermal energy absorbed by the collector is sufficient to compensate for heat losses to the surrounding environment. The limited fluctuations observed during this period indicate good thermal stability, which is advantageous for maintaining a consistent thermal output. Such stability is particularly desirable in solar thermal applications because it enhances the efficiency and reliability of the system. After 17:00, the temperature begins to decrease gradually. From about 35 °C at 17:00, it falls progressively to around 24 °C by 18:00. This decline corresponds to the reduction in solar irradiance as the sun approaches the horizon. Since the amount of incoming solar energy decreases, heat losses become dominant, leading to a gradual cooling of the

collector. Overall, the curve demonstrates that the collector is capable of achieving and maintaining relatively high temperatures for a significant portion of the day. The temperature remains above 30 °C for several hours, indicating effective solar energy capture and storage. The difference between the minimum and maximum temperatures is approximately 13 °C, reflecting the daily thermal variation experienced by the system.

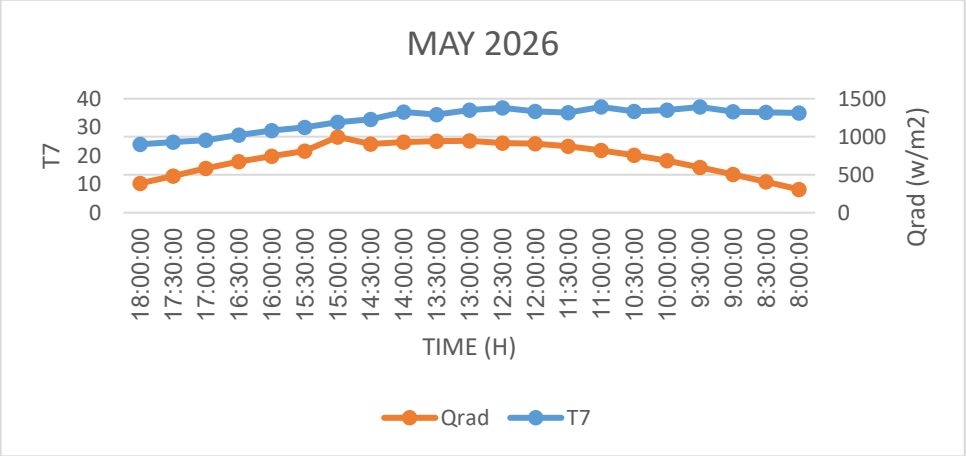


Fig. III .20: Hourly Variation of Solar Radiation (Q_{rad}) and Temperature (T_7) - May 2026

An academic analysis reveals a diurnal thermodynamic study from May 2026 tracking solar irradiance (Q_{rad}) and a localized temperature metric ($T7$). Crucially, the x-axis is inverted, requiring a right-to-left chronological reading from 8:00 to 18:00 to properly evaluate the system's behavior. In the morning, Q_{rad} rises steadily from 300 W/m^2 toward a stable midday plateau near 900 W/m^2, while $T7$ displays strong thermal inertia by maintaining a steady baseline between 35°C and 37°C. A notable anomaly occurs at 15:00, where Q_{rad} suddenly spikes to its peak of 1000 W/m^2 just as $T7$ experiences a sharp transient dip down to 31°C – 32°C, an inverse coupling likely driven by environmental factors like sudden wind or cloud dynamics. As evening approaches, both variables rapidly decline toward 18:00, though for standard academic presentation, the chronological sequence of the x-axis should be reversed to comply with standard data visualization norms.

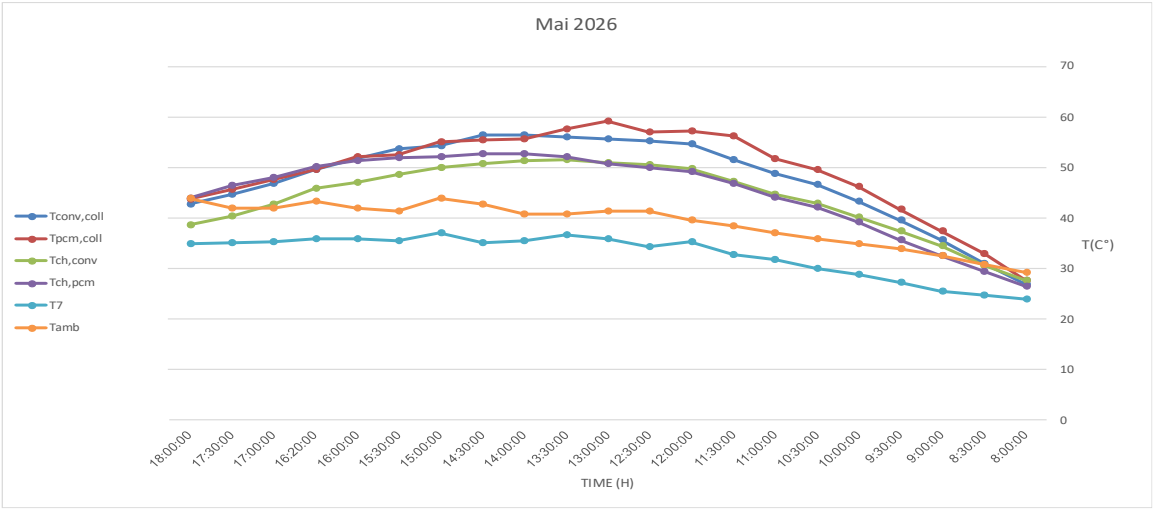


Fig. III .21: Experimental Temperature Evolution of a Solar Collector Integrated with Phase Change Material (PCM) vs. Conventional System

the chart evaluates a PCM-enhanced solar collector against a conventional setup from 08:00 to 18:00 (ordered right to left) in May 2026. While the ambient temperature (T_{amb}) peaks near 43°C at 15:00 and T_7 serves as a stable baseline, the conventional collector ($T_{conv,coll}$) heats up rapidly during the morning. By midday, the PCM collector ($T_{pcm,coll}$) achieves a higher peak of approximately 60°C. Crucially, the PCM channel temperature ($T_{ch,pcm}$) exhibits a distinct thermal plateau between 10:00 and 13:00, indicating latent heat absorption during phase transition. In the afternoon, as sunlight fades and the conventional channel ($T_{ch,conv}$) drops rapidly, the PCM system exhibits a clear thermal lag, maintaining a prolonged, higher heat output that successfully extends useful thermal energy availability into the evening.

- **Analysis of orange slice drying kinetics**

For dehydrated orange slices, the drying model was predicted using the moisture ratio (MR). The statistical outcomes of the air-drying process in the two drying systems (with and without PCM) are described in Table 3. The optimal model was selected based on its correlation coefficient R^2, sum of squares error (SSE), and root mean square error (RMSE) metrics. The logarithmic model was found to have the highest correlation coefficient (R^2) value and the lowest SSE and RMSE values, making it the most effective representation of the orange-slice drying process in the two drying systems.

The MATLAB R2016 program was used for regression analysis, with model adequacy determined by the correlation coefficient. The logarithmic model exhibited the highest correlation coefficient (R^2) value and the lowest SSE and RMSE values, making it the most

effective representation of the orange-slice drying process across the two drying systems. Notably, among these configurations, the drying system with PCM achieved the best coefficients, including R^2 = 0.9964, RMSE = 0.0178, and SSE = 0.0060. Table III.4 presents the statistical findings for various thin-layer drying models of the two drying systems. Fig. III.22 shows the moisture ratio (w.b.) of orange slices during the drying process over time for the two drying systems. The moisture ratio values, recorded from 08:00 to 17:00, provide a comprehensive assessment of the drying kinetics. Both dryers exhibit a decreasing trend in MR; however, the moisture removal rates differ significantly among the configurations. In the system with PCM, the moisture ratio decreased sharply after 1:00 PM, falling below 0.01 by 3:30 PM. The system without PCM exhibited a slower drying rate; its MR declined gradually and remained higher throughout the process, failing to reach below 0.01 by 17:00 h.

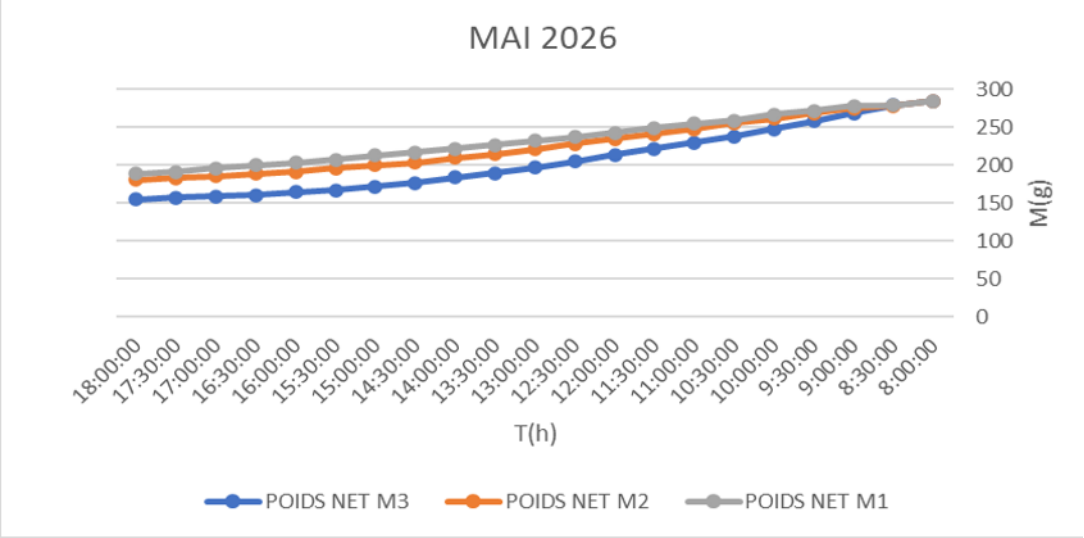


Fig III.22:Moisture content (w.b.) reduction of orange slices during the drying process over time.

Table III.4: Statistical results for different thin-layer drying models for orange slices.

Model	Constants				R^2	RMSE	SSE
	1	2	3	4			
Newton	0,4113	-	-	-	0,9883	0,0324	0,0199
Page	0,3391	1,1714	-	-	0,9946	0,0219	0,0091
Henderson & Pabis	1,0280	0,4220	-	-	0,9891	0,0312	0,0185
Logarithmic	**1,0730**	**0,3481**	**-0,0716**	**-**	**0,9964**	**0,0178**	**0,0060**
Two-Term	8,827E-05	0,4247	1,02813	0,4223	0,9891	0,0312	0,0185

III.7. Conclusion:

This chapter presents a comprehensive analysis of two prototype indirect solar dryers (ISDs) designed for non-renewable energy contexts in the Algerian Valley, focusing on their operational processes, experimental performance, and mathematical modeling. A comparative assessment is conducted between a standard stationary unit and an enhanced system integrated with a phase-change material (PCM)-comprising a paraffin wax and aluminum shavings mixture—to improve thermal storage capabilities. Both insulated systems were tested within a UDERZA unit during the hot summer months, targeting the drying of high-moisture sheets under controlled airflow conditions, with optimized mesh trays and a fan facilitating rapid humidity regulation. The PCM-assisted collector achieved operating temperatures of up to 60°C while effectively storing thermal energy during morning solar exposure. Moreover, a novel thermostatic composite material was developed, which not only retained accumulated heat but also provided superior thermal insulation, thereby extending the drying process well into the evening hours. To complete the analysis, three strategic kinetic models for diffusion were established, incorporating key statistical indicators such as (RMSE, X^2,R^2),and RMSE, alongside the application of Fick's laws to quantify internal moisture diffusion and ratio contributions.

General Conclusion

This thesis presents a comprehensive investigation into the drying kinetics of orange slices using an indirect solar dryer operated under forced convection, with experiments conducted during the harsh summer of 2026 in El-Oued, Algeria. The primary objective was to develop a sustainable post-harvest preservation method capable of mitigating the inherent intermittency of solar radiation. To this end, a comparative analysis was carried out between a conventional solar collector and an enhanced prototype integrating a thermal storage system. The innovative design employed a composite phase change material composed of Egyptian paraffin wax and highly conductive aluminum shavings (PCM-ALSH), which effectively overcame the poor thermal conductivity of pure paraffin. Empirical results revealed that the PCM-ALSH collector achieved a superior thermal peak of up to 60°C.

During the solidification phase, the composite material produced a pronounced thermal lag, functioning as an efficient buffer that smoothed temperature fluctuations and sustained the delivery of hot air to the drying chamber well after sunset. Consequently, the hybrid system extended active drying operations by up to eight hours beyond daylight, reducing the total dehydration time from 32 to 26 hours, a notable 30% improvement. Importantly, the regulated thermal environment helped preserve the structural integrity, nutritional content, and sensory attributes of the dried orange slices.

Lower and more stable temperatures minimized adverse reactions such as non-enzymatic browning, while vitamin degradation and aroma loss were significantly curtailed compared to traditional open-air sun drying.For mathematical validation, several thin-layer drying modelsincluding Page, Henderson and Pabis, and Lewis, were fitted to the experimental data, all demonstrating strong statistical correlation, as confirmed by high (R^2) and (X^2) and (RMSE) values. Furthermore, Fick's second law of diffusion was successfully applied to estimate the effective moisture diffusivity (D_{eff}), providing crucial parameters for future system scaling and optimization.

Overall, the integrated PCM-ALSH solar dryer presents a highly efficient, reliable, and environmentally friendly solution tailored to desert agriculture, reducing food waste, lowering dependence on fossil fuels, and offering economic benefits to local farmers. Future research should extend these findings through multi-seasonal field trials to verify operational stability, alongside comprehensive exergy and enviro-economic analyses to assess commercial feasibility. Additional improvements, such as optimizing air flow rates or incorporating dehumidification units, could further enhance drying performance. Exploring cost-effective and eco-friendly alternative phase change materials would also help reduce initial investment costs for rural communities. In conclusion, this study lays a robust and scalable foundation for the

application of green energy technologies in food preservation, with significant potential for broader adoption in arid regions.

Bibliographicalreferences

[1] D. Rabha and P. J. S. e. Muthukumar, "Performance studies on a forced convection solar dryer integrated with a paraffin wax–based latent heat storage system," vol. 149, pp. 214-226, 2017.
[2] W. B. Chaouch, A. Khellaf, A. Mediani, M. E. A. Slimani, A. Loumani, and A. J. S. E. Hamid, "Experimental investigation of an active direct and indirect solar dryer with sensible heat storage for camel meat drying in Saharan environment," vol. 174, pp. 328-341, 2018.
[3] D. Singh, P. J. E. S. Mall, Part A: Recovery, Utilization,, and E. Effects, "Experimental investigation of thermal performance of indirect mode solar dryer with phase change material for banana slices," vol. 46, no. 1, pp. 15268-15285, 2020.
[4] H. Krabch, R. Tadili, and A. J. R. i. E. Idrissi, "Design, realization and comparison of three passive solar dryers. Orange drying application for the Rabat site (Morocco)," vol. 15, p. 100532, 2022.
[5] J. M. Panchal, K. V. Modi, S. B. Chaudhary, P. B. Jadeja, and V. J. Patel, "Comparative experimental analysis of potato slice drying using a multiple phase change material cascaded modified indirect solar dryer and conventional indirect solar dryer," *Journal of Energy Storage,* vol. 67, p. 107644, 2023.
[6] K. Xu *et al.*, "Simulation optimization and energy consumption evaluation on the wood solar drying kiln with heat storage and dehumidification system," *Applied Thermal Engineering,* vol. 240, p. 122262, 2024.
[7] M. Murthi, P. M. Kumar, S. K. Bandili, P. Johnson, M. J. T. o. E. S. Sakthivel, and E. Applications, "Study on an indirect solar dryer for drying sliced bitter gourd using PCM," vol. 6, no. 1, pp. 1-14, 2025
[8] N. Meneceur, I. Bouaziz, K. Aliouat, K. Deghoum, and Y. Aoun, "Design and evaluation of an indirect solar dryer with a phase change material-integrated collector for thermal energy storage," *Journal of Stored Products Research,* vol. 117, p. 103015, 2026.
[9] Design and Experimental Analysis of a Direct Solar Dryer with Thermal Energy Storage Equipped with a New Heat Recovery System, KasdiMerbah University– Ouargla
[10] . Abdelouahab, B., Y. Naiti, and K.i.e. Melouah, Conception, fabrication et investigation expérimentale d'un dispositif de stockage d'énergie thermique par matériau à changement de phase couplé avec un séchoir solaire de type serre, in Département de Génie Mécanique - Master. 2022, UNIVERSITE KASDI MERBAH – OUARGLA.
[11] . HADJAIDJI, N. and A.D. GOUSSEUM, Design and Experimental Analysis of a Direct Solar Dryer with Thermal Energy Storage Equipped with a New Heat Recovery System. UNIVERSITE KASDI MERBAH OUARGLA.
[12] . Belessiotis, V. and E. Delyannis, Solar drying. Solar Energy, 2011. **85**(8): p. 1665- 1691.
[13] Contribution à l'étude d'amélioration des performancesthermiques des séchoirs solaires utilisant différentes techniquesd'apport de chaleur, in GENIE MECANIQUE. 2019University KasdiMerbah Ouargla: SCIENCES APPLIQUEES.
[14] Handbook of Industrial Drying, ed. A.S.M. (editor). Vol. 1279. 2006, by Taylor & Francis Group, LLC.: by Taylor & Francis Group, LLC. 1279.
[15] Nnamchi, O., et al., Solar dryers: A review of mechanism, methods and critical analysis of transport models applicable in solar drying of product. Green Energy and Resources, 2025. **3**(2): p. 100118.

[16] D Pagukuman, B.N., A review of the significant effect of external factors of the solar dyer design to dried foods product quality. Journal of Engineering, Design, and Technology, 2021. ahead-of-print.

[17] A Parametric Study on the Effect of Drying Performance ofSolar Dryer integrated with a Dehumidifier Unit.

[18] Shekata, G.D., G.S. Tibba, and A.T. Baheta, Recent advancements in indirect solar dryer performance and the associated thermal energy storage. Results in Engineering, 2024. **24**: p. 102877.

[19] Benli, H., Energetic performance analysis of a ground-source heat pump system with latent heat storage for greenhouse heating. Energy conversion management, 2011.**52**(1): p. 581-589.

[21] BOUBEKRI, A., D. MENNOUCHE, and T. HADIBI, Experimental study of a solar drying process with improved thermal performances, in Department of Mechanical Engineering. 2021, KasdiMerbah University – Ouargla.

[22] Lashin, A. and N. Al Arifi, Geothermal energy potential of southwestern of Saudi Arabia" exploration and possible power generation": A case study at Al Khouba area– Jizan. Renewable Sustainable Energy Reviews, 2014. 30: p. 771-789.

[23] Fudholi, A., et al., Review of solar dryers for agricultural and marine products. Renewable and Sustainable Energy Reviews, 2021. 14: p. 1-30.

[24] Rathore, G., et al., Recent Progress in Solar Dryers using Phase Changing Material: A Review. Journal of the Korean Society of Mineral and Energy Resources Engineers, 2023. **2**: p. 57-77.

[25] Naderinezhad, S., et al., Mathematical modeling of drying of potato slices in a forced Convective dryer based on important parameters. 2016. 4(1): p. 110-118.

[26] Crank, J., The mathematics of diffusion. 1979: Oxford University press.

[27] Lewis, W.K.J.I. and E. Chemistry, the rate of drying of solid materials. 1921.

[28] Page, G.E., Factors Influencing the Maximum Rates of Air-Drying Shelled Corn in Thin layers. 1949: Purdue University.

[29] Henderson, S.J.J.A.E.R., Grain drying theory, I. Temperature effect on drying coefficient. 1961.

[30] Midilli, A., K. HAYDAR, and Y.J.A.n.m.f.s.-l.d.D.T. Zİ, Yapar. 2002

[31] Dr. Saad Ahmed Saad Halbo, Dr. Adel Zaki Mohamed Badie, Dr. Mahmoud Ali Ahmed Bakheet, Food Industry Technology, 2008. Foundations of Food Preservation and Processing. Publisher: The Academic Library, an Egyptian joint-stock company

[32] boumediene TOUATI) etude théorique et expérimentale du séchage solaire des feuilles de la menthe verte (thése de doctorat. Université abdoubekerbelkaid ; tlemcen 2008.

[33] philippedudez ,andréthémeilin et max reynes(le séchage solaire a petite échelle des fruitse et légumé)guidepratique .paris France 1991

[34] Yves JANNOT, "Thermique Solaire", edilivre, France, (Janvier 2007).

[35] M.A. Leon, S. Kumar, S.C. Bhattacharya, 2002. A comprehensive procedure for performance evaluation of solar food dryers. Renewable and Sustainable Energy Reviews6 . .393-367

[36] W. E. Mehling, C. Price, J. J. Daubenmier, M. Acree, E. Bartmess, and A. J. P. o. Stewart, "The multidimensional assessment of interoceptive awareness (MAIA)," vol. 7, no. 11, p. e48230, 2012.

[37] M. A. Kherrafi *et al.*, "Advancements in solar drying technologies: Design variations, hybrid systems, storage materials and numerical analysis: A review," vol. 270, p. 112383, 2024.

[38] S. Singh, H. S. J. A. Singh, and I. Research, "RELATIONSHIP BETWEEN CONSUMER SATISFACTION, MALL ENVIRONMENT, SHOPPING MOTIVATION, AND FREQUENCY OF VISITS TO SHOPPING MALLS IN LUCKNOW," 2025.

[39] S. Simal, A. Femenia, M. C. Garau, and C. Rosselló, “Use of exponential, Page’s and diffusional models to simulate the drying kinetics of kiwi fruit,” J. Food Eng., vol. 66, no. 3, pp. 323–328, Feb. 2005

[40] G. Y. Wang and R. Singh, “SINGLE LAYER DRYING EQUATION FOR ROUGH RICE.,” 1978.

[41] W. K. Lewis, “The Rate of Drying of Solid Materials,” Ind. Eng. Chem., vol. 13, no. 5, pp. 427–432, May 1921.

[42] B. K. Bala and J. L. Woods, “Thin layer drying models for malt,” J. Food Eng., vol. 16, no. 4, pp. 239–249, Jan. 1992.

[43] R. Dandamrongrak, R. Mason, and G. Young, “The effect of pretreatments on the drying rate and quality of dried bananas,” Int. J. Food Sci. Technol., vol. 38, no. 8, pp. 877–882,

[44] Dec. 2003.

[45] M. D. Buser, M. L. Stone, G. H. Brusewitz, N. O. Maness, and D. P. Whitelock, “THINLAYER DRYING OF MARIGOLD FLOWERS AND FLOWER COMPONENTS FOR
PETAL REMOVAL,” Trans. ASAE, vol. 42, no. 5, pp. 1367–1374, Sep. 1999.

[46] G. E. PAGE, “FACTORS INFLUENCING THE MAXIMUM RATES OF AIR DRYING SHELLED CORN IN THIN LAYERS.,” Theses Diss. Available from ProQuest, Jan. 1949.

[47] M. Kashaninejad, A. Mortazavi, A. Safekordi, and L. G. Tabil, “Thin-layer drying characteristics and modeling of pistachio nuts,” J. Food Eng., vol. 78, no. 1, pp. 98–108, Jan. 2007.

[48] S. M. Hendorson, “Grain Drying Theory (I) Temperature Effect on Drying Coefficient,” J. Agric. Eng. Res., 1961.

[49] P. C. Panchariya, D. Popovic, and A. L. Sharma, “Thin-layer modelling of black tea drying process,” J. Food Eng., vol. 52, no. 4, pp. 349–357, May 2002.

[50] G. N. Lewis, M. Randall, K. S. (Kenneth S. Pitzer, and L. Brewer, “Thermodynamics,” p. 723.

[51] G. P. Sharma and S. Prasad, “Effective moisture diffusivity of garlic cloves undergoing microwave-convective drying,” J. Food Eng., vol. 65, no. 4, pp. 609–617, Dec. 2004.

[52] A. Vega-Gálvez, R. Lemus-Mondaca, C. Tello-Ireland, M. Miranda, and F. Yagnam, “Estudio de la cinética del secado convectivo de arándano variedad O?Neil (Vaccinium corymbosum L.),” Chil. J. Agric. Res., vol. 69, no. 2, pp. 171–178, 2009.
[53] A. Midilli and H. Kucuk, “Mathematical modeling of thin layer drying of pistachio by using solar energy,” Energy Convers. Manag., vol. 44, no. 7, pp. 1111–1122, May 2003.
[54] L. R. Verma, R. A. Bucklin, J. B. Endan, and F. T. Wratten, “Effects of Drying Air Parameters on Rice Drying Models,” Trans. ASABE, vol. 28, no. 1, pp. 296–301, Jan. 1985.
[55] N. A. Goyalde, E. C. Melo, R. P. Rocha, A. L. D. Goneli, and F. L. Araújo, “MATHEMATICAL MODELING Of THE DRYING KINETICS OF SUGARCANE SLICES,” Rev. Bras. Prod. Agroindustriais, vol. 11, no. 2, pp. 117–121, Dec. 2009
[56] B. Vasić, A. Zurutuza, and R. J. C. Gajić, "Spatial variation of wear and electrical properties across wrinkles in chemical vapour deposition graphene," vol. 102, pp. 304-310, 2016.
[57] J. Crank, R. S. J. I. J. o. H. Gupta, and M. Transfer, "Isotherm migration method in two dimensions," vol. 18, no. 9, pp. 1101-1107, 1975.